NATIONAL AERONAUTICS AND SPACE ADMINISTRATION

Technical Report 32-1505

Addendum

Satellite Auxiliary-Propulsion Selection Techniques

Survey of Auxiliary Electric Propulsion Systems

Lee B. Holcomb

JET PROPULSION LABORATORY
CALIFORNIA INSTITUTE OF TECHNOLOGY
PASADENA, CALIFORNIA

July 15, 1971

NATIONAL AERONAUTICS AND SPACE ADMINISTRATION

Technical Report 32-1505

Addendum

Satellite Auxiliary-Propulsion Selection Techniques

Survey of Auxiliary Electric Propulsion Systems

Lee B. Holcomb

JET PROPULSION LABORATORY
CALIFORNIA INSTITUTE OF TECHNOLOGY
PASADENA, CALIFORNIA

July 15, 1971

Prepared Under Contract No. NAS 7-100
National Aeronautics and Space Administration

Preface

The work described in this report was sponsored by the NASA/OSSA Applications Technology Satellites Program Office and was performed by the Propulsion Division of the Jet Propulsion Laboratory.

Acknowledgment

The author would like to acknowledge the cooperation of the many corporations, NASA, and other government agencies for permission to reproduce photographs and data, and for freely discussing various technical areas. During the preparation of the manuscript, the author had the benefit of critical reviews of various chapters by C. Dulgeroff, J. Hyman, and H. J. King of Hughes Research Laboratories; R. M. Worlock of Electro-Optical Systems; S. Zafran of TRW Systems Group; G. Seikel and S. A. Burkhart of NASA Lewis Research Center; and W. J. Guman of Fairchild-Hiller. The author would further like to acknowledge the continuous assistance of J. H. Kelley, D. J. Kerrisk, T. D. Masek, and N. Nerheim.

Contents

Contents (contd)

Tables

Figures

Contents (contd)

Figures (contd)

Abstract

A review of electric thrusters for satellite auxiliary propulsion was conducted at JPL during the past year. Comparisons of the various thrusters for attitude propulsion and east-west and north-south stationkeeping were made based upon performance, mass, power, and demonstrated life. Reliability and cost are also discussed. The method of electrical acceleration of propellant served to divide the thruster systems into two groups: electrostatic and electromagnetic. Ion and colloid thrusters fall within the electrostatically accelerated group while MPD and pulsed plasma thrusters comprise the electromagnetically accelerated group. The survey was confined to research in the United States with accent on flight and flight prototype systems.

Satellite Auxiliary-Propulsion Selection Techniques

Survey of Auxiliary Electric Propulsion Systems

I. Introduction

With the success of the experimental electric thrusters that are on board the Application Technology Satellite (ATS) IV, Lincoln Experimental Satellite (LES) 6, and Space Electric Rocket Test (SERT) II, along with the applications of state-of-the-art electric propulsion technology to LES 8 and ATS F and G, auxiliary electric propulsion is emerging from experimental to flight status. The satellite auxiliary propulsion designer is now faced with the evaluation of present state-of-the-art auxiliary electric thrusters for application to unmanned satellites, particularly long-life synchronous satellites. The purpose of this addendum is to provide program managers and systems engineers with comparative information on auxiliary electric propulsion systems.

A detailed selection method was presented in JPL TR-1505, *Satellite Auxiliary Propulsion Selection Techniques*, in November 1970. The thrusters surveyed in that report were limited to those that rely on gasdynamic pressure forces to accelerate propellant, e.g., chemical and inert gas. Electric thrusters surveyed herein rely on electrostatic or electromagnetic forces to accelerate propellant. The varied characteristics of electric thrusters separate these devices into distinct classes. Ion and colloid thrusters comprise the electrostatically accelerated group while magnetoplasmadynamic (MPD) and pulsed plasma thrusters comprise the electromagnetically accelerated group.

The discussion in this addendum is divided into five sections for each of the four thruster types:

(1) General description of the thruster.

(2) Early history of thruster development.

(3) Discussion of thruster characteristics.

(4) Space flight experience.

(5) Survey of state-of-the-art thrusters.

The thrusters discussed were developed by the Hughes Research Laboratory (HRL), Malibu, Calif.; Electro-Optical Systems (EOS), Pasadena, Calif.; Fairchild-Hiller Corporation, Farmingdale, N.Y.; TRW Systems Group, Redondo Beach, Calif.; NASA Lewis Research Center (LeRC), Cleveland, Ohio; General Electric Company, Space Division, Philadelphia, Pa.; and Cornell Aeronautical Laboratories, Buffalo, N.Y.

These discussions are followed by comparisons of surveyed thrusters for use on satellites, to provide east-west and north-south stationkeeping.

II. Ion Thrusters

A. What Is an Ion Thruster?

The ion thruster is defined as a device that electrostatically accelerates charged single atoms or ions. Ion thrusters may be categorized according to the process by which the ions are produced. Bombardment ionization results from the collision of an electron with a single propellant atom in the gaseous phase. Contact ionization is an interaction between a single propellant atom and a heated surface of a metal with a high work function. These sources are sufficiently different in their operational requirements and in the nature of the ion beam they produce to influence the design of other elements in the accelerator and the design of the electric power supply required. Ion engines are therefore normally classified in terms of their source: contact-ion thrusters and electron-bombardment thrusters.

A conceptual diagram of a contact-ion thruster is presented in Fig. 1. Liquid cesium propellant is fed to a vaporizer by capillary action. The Cs vapor produced at a pressure of less than 7×10^{1} N/m^2 (1 psia) flows through a heated porous tungsten ionizer (877–1077°C), and contact ionization proceeds with 99–100% effectiveness.[1] The ionizer is maintained at a voltage V_A above spacecraft potential and the accelerator electrode is maintained at a voltage V_B below spacecraft potential to preclude electron migration (from neutralizer) into the acceleration gap and provide sufficient potential gradient for proper ion focusing. The ratio of beam power to thrust is proportional to specific impulse (I_{sp}); therefore, thruster power requirements can become excessive at high specific impulse (high exhaust speeds). A decelerator electrode is sometimes provided. During thruster operation, positive ions are being emitted from the device; hence, if no provision for neutralization of the ion beam were made, the spacecraft would acquire a negative potential. The ion exhaust beam is neutralized by electrons (electrons drawn into beam by positive ions) supplied from a thermionic filament or plasma bridge neutralizer.

Principles of operation of the electron-bombardment thruster are shown in Fig. 2. Liquid cesium or mercury propellant is fed to a vaporizer. The propellant vapor produced is then fed to a discharge chamber. Electrons are emitted from the cathode and spiral about magnetic

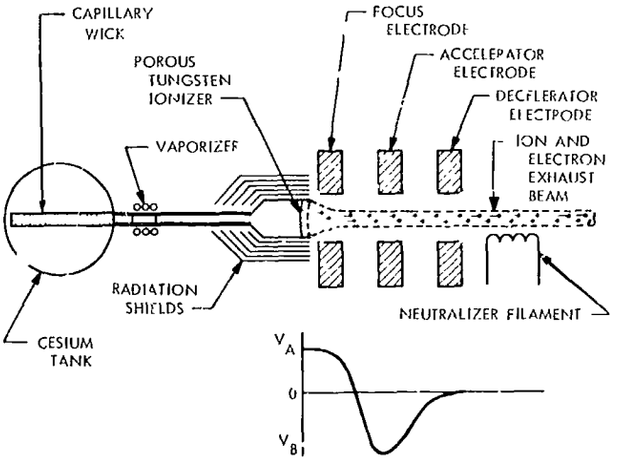

Fig. 1. Conceptual diagram of the contact-ion thruster

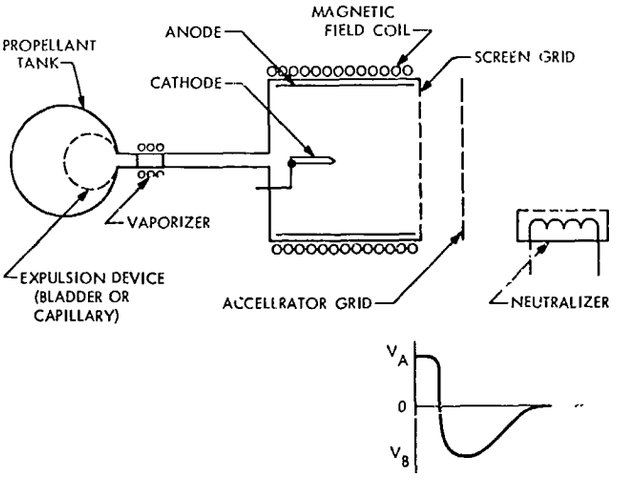

Fig. 2. Conceptual diagram of the electron-bombardment thruster

field lines in the discharge chamber. Electrons suffer collisions with propellant in the discharge chamber and ions are formed. Cathode configurations differ between designs; however, a hollow cathode with a fraction (10–100%) of the propellant flowing through it has been incorporated in most recent electron-bombardment ion discharge chambers. Anode-magnet configurations differ between thruster designs, with the simplest arrangement presented in Fig. 2. Most discharge chambers have a screen to provide a physical surface to which the plasma boundary can attach itself. The accelerator and neutralizer of the electron-bombardment thruster are similar to those discussed in the contact-ion thruster system.

[1]Effectiveness in this sense means percent of propellant flow ionized.

B. History of Ion Thrusters

Two pioneers of rocketry were Robert H. Goddard and Hermann Oberth. The earliest known record of the idea of electric propulsion for rocket vehicles appears in the notebook of R. H. Goddard (Ref. 1). The thought occurred to Goddard that electrostatically repelled particles might be the answer to the problem of obtaining high exhaust velocities at bearable chamber temperatures. Hermann Oberth consolidated much of his thoughts on rocket propulsion in the book *Wege zur Raumschiffahrt* (Ref. 2). One section of that book is devoted to electric propulsion. A more detailed history of early electric propulsion studies is presented in Ref. 3 by Ernst Stuhlinger.

Many studies of ion thrusters for spacecraft were performed from 1940 to 1957. In 1957 the studies of electric propulsion increased in number; more specific problems were tackled, and the Air Force's Office of Scientific Research began funding research in this field. By 1958 many companies were investigating ion thrusters. Rocketdyne, a division of North American Aviation, developed the first experimental ion thruster in August 1958 (Refs. 4, 5, and 6). Electro-Optical Systems (EOS) followed with another thruster in January 1959 (Ref. 7). Both General Electric and Thompson Ramo-Woodridge operated ion motors in 1959 (Refs. 8 and 9). At the Lewis Flight Laboratory of the National Advisory Committee for Aeronautics (NACA), the electron-bombardment thruster was developed and operational by 1960 (Ref. 10). As early as 1960 the Hughes Aircraft Company began applying a particle trajectory analogue simulator to the problems of beam formation and beam neutralization (Ref. 11).

C. Characteristics of Ion Thrusters

In 1913, Langmuir (Ref. 12) demonstrated that a heated surface of a metal of high electronic work function ϕ immersed in the vapor of an alkali metal of ionization potential (ϵ_i) lower than the surface work function would convert some of the alkali atoms to positive ions. Several metal surface and alkali metal vapor combinations produce this effect; however, the best ion source has proved to be a tungsten surface and cesium vapor combination. The porous tungsten ionizer operates at approximately 1050°C, and is the source of a constant heat loss (radiation) to space. As beam power is decreased (a decrease in beam power corresponds to a decrease in I_{sp}), the fixed ionizer power becomes predominant. A typical curve of power-to-thrust ratio as a function of specific impulse is presented in Fig. 3. As specific impulse decreases below 49,000 N-s/kg (5000 lbf-s/lbm), the power-to-thrust ratio begins to increase, because of the constant ionizer power requirement. Contact-ion thruster power requirements for a given thrust level reach a minimum at a specific impulse of about 49,000 N-s/kg (5000 lbf - s/lbm).

A major limitation of ion thrusters is accelerator electrode erosion caused by ion bombardment. The ions that cause most of the damage are those formed from neutral particles that pass through the ionizer, and have subsequently undergone charge exchange collisions with fast positive ions. Therefore, a high-ionization efficiency (i.e., percent of propellant flow ionized) is important in extending electrode life. The cesium contact-ionization thruster is characterized by high-ionization efficiency (99–100%); this feature is partially offset by the high current density of the cesium contact thruster beam.

A great number of cesium contact thrusters have been fabricated and tested. Two basic types have evolved: "button" thrusters, and "strip" thrusters; these titles refer to the ionizer geometry. The button cesium contact thruster employs a circular porous tungsten "button" ionizer, while the strip contact thruster employs a long thin porous tungsten "strip" ionizer. The button contact thrusters have been designed for 0 to 89-μN (0 to 20-μlbf) thrust while strip contact thruster designs range in thrust level from 444 μN to 96.8 mN (100 μlbf to 21.8 mlbf).

Several types of thrust vectoring are available to cesium contact thrusters; however, the most widely used concept

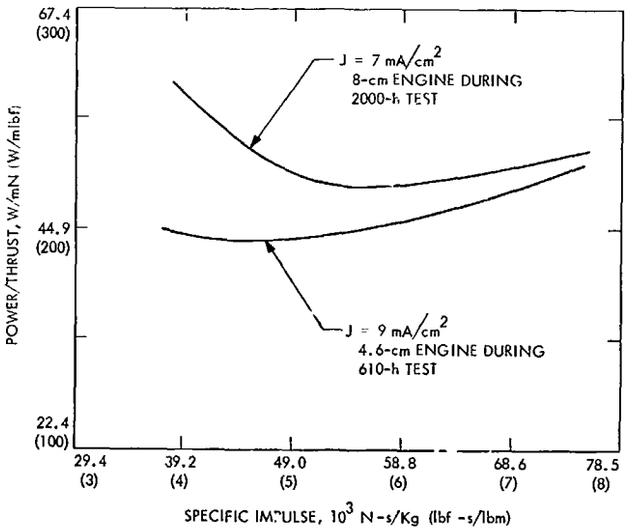

Fig. 3. Power-to-thrust vs specific impulse for contact-ion thrusters (Ref. 19)

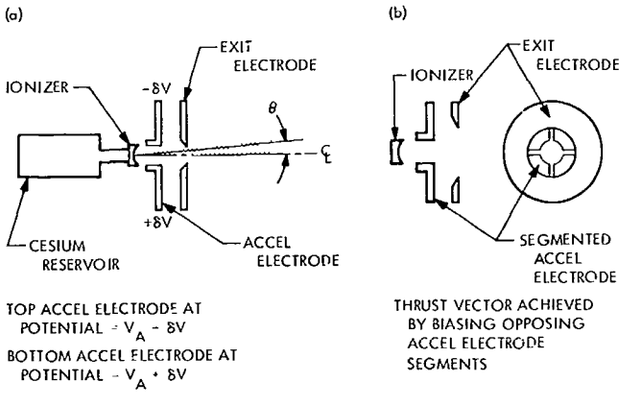

Fig. 4. Electrostatic beam deflection (a) of a linear strip contact-ion thruster, and (b) of a button contact-ion thruster

is electrostatic beam vectoring. A small bias may be placed on opposite sides of a linear accelerator electrode as in Fig. 4a. A similar scheme is applicable to circular button-type cesium contact thrusters as in Fig. 4b.

In November, 1960, Harold R. Kaufman presented a paper on ion rockets employing electron-bombardment ion sources (Ref. 10). This device later became known as the Kaufman thruster; however, the early Kaufman thruster was quite different from the experimental mercury electron-bombardment thruster on SERT II. The early thrusters employed a thermal filament (cathode) at the center of the ionization chamber (see Fig. 5). Electrons, emitted by the filament are caused to spiral about magnetic field lines caused by a weak axial magnetic field, thus forcing the electrons to collisional dominated diffusion. Recently, hollow cathodes have replaced thermal filament cathodes in electron-bombardment thrusters. The comparable performance, increased propellant utilization, and decreased heater power of hollow cathodes favor this replacement. Discharge chamber geometry of electron-bombardment thruster designs has also seen some changes, including magnet geometry (Fig. 6).

Although the electron-bombardment thruster has been operated with several propellants, mercury and cesium are the most common. The ionization potential for cesium is less than that of mercury; however, the cross section for electron-atom interactions for mercury is greater than for cesium. The result is that either propellant is as easy to ionize. Mercury with its larger molecular weight and increased density will have the advantages of increased thrust and decreased tankage weight. Cesium will wet flow passages better than mercury; therefore voltage

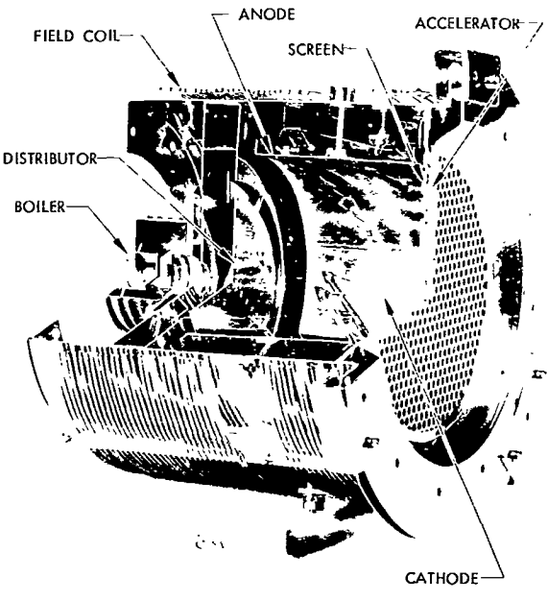

Fig. 5. Early Kaufman mercury electron-bombardment thruster (photo courtesy of NASA LeRC)

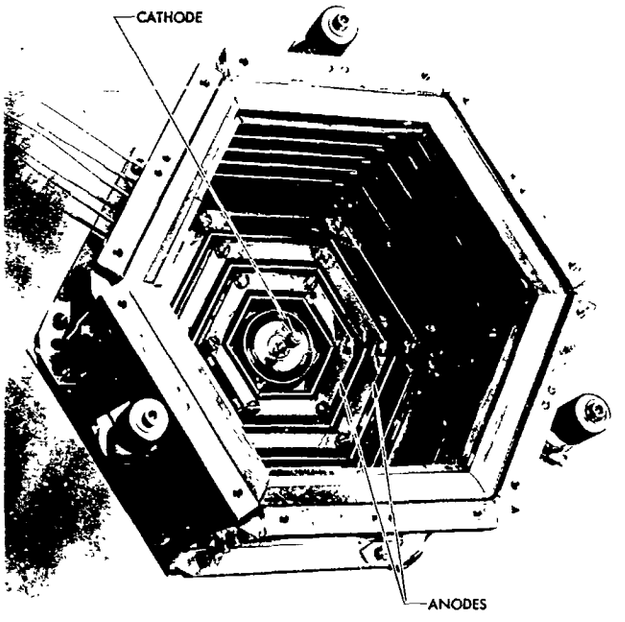

Fig. 6. Discharge chamber geometry of the EOS magneto-electrostatic containment (MESC) thruster (photo courtesy of EOS)

isolation of a cesium propellant tank, which would allow a common tank for several thrusters, becomes difficult. An isolator for mercury-bombardment thrusters has been developed.

Mercury and cesium bombardment thrusters differ in the design of their discharge chambers, cathodes, and accelerator electrodes. Differences in thruster design lead to differences in propellant utilization efficiency. As was pointed out earlier, accelerator electrode lifetime is a strong function of propellant utilization efficiency. High propellant utilization efficiency must be balanced against discharge chamber power. Curves of discharge chamber losses (J/Ion) as a function of propellant utilization efficiency (Fig. 7) usually have a break around 85 to 95% propellant utilization efficiency. The desired operation is at this break, because increased discharge chamber losses add a fixed increase to thruster total power.

The low-fixed discharge chamber power requirements of an electron-bombardment thruster, compared to high-fixed radiation loss from the hot ionizer of a contact-ion thruster, suggests a somewhat lower optimum specific impulse for the electron-bombardment thruster. This is displayed in Fig. 8, with the power-to-thrust ratio minimum at 29,420 to 39,200 N-s/kg (3000 to 4000 lbf-s/lbm).

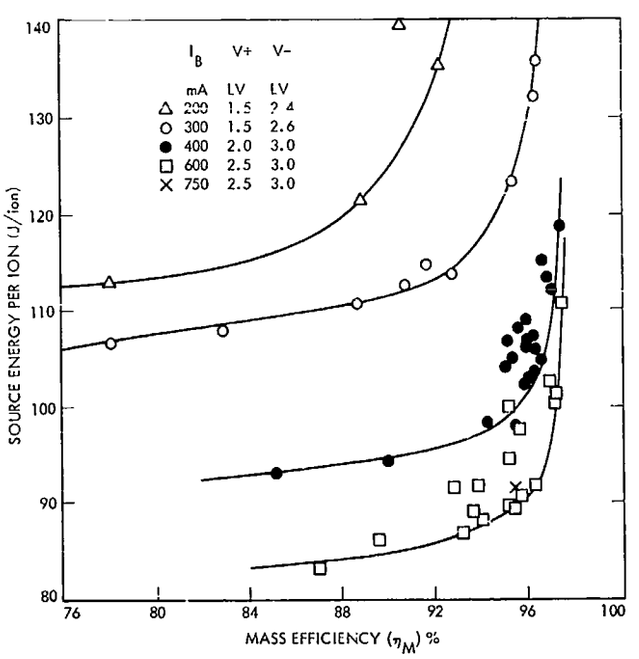

Fig. 7. Discharge chamber power as a function of mass utilization efficiency (Ref. 25)

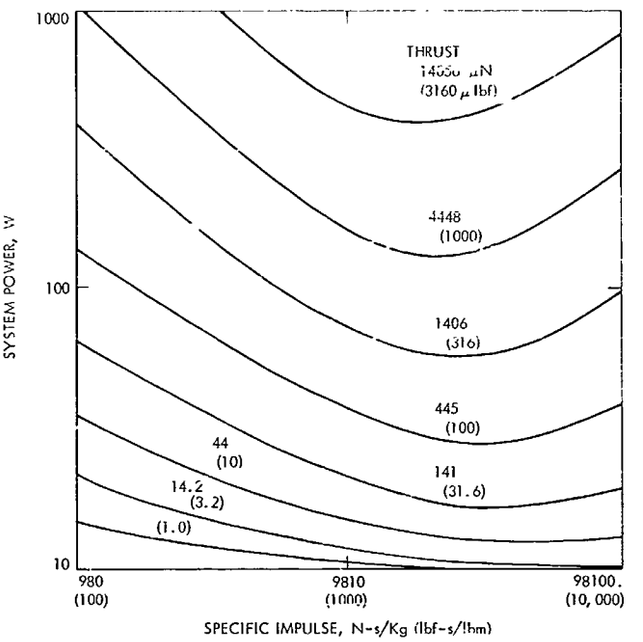

Fig. 8. Effect of system power and thrust on optimum specific impulse of electron-bombardment thrusters (Ref. 20)

Cesium contact thrusters rely primarily on electrostatic beam deflection for thrust vectoring, while electron-bombardment systems utilize mechanical grid movement, electrostatic beam deflection, or mechanical thruster movement for thrust vectoring. One method of beam deflection (electrostatic) is presented in Fig. 9a. The accelerator grid is segmented and contained in a glass coating that separates the positive discharge chamber plasma from the accelerator electrode. A small bias may be placed on opposite sides of the accelerator electrode to achieve electrostatic beam deflection. Mechanical grid movement has been used for thrust vectoring of electron-bombardment ion engines. The physical effects of accelerator grid translation on beam deflection are indicated in Fig. 9b. Grid translation can be implemented by use of thermal expansion forces, created by electrically heated grid supports. Also, mechanical thruster gimbaling has been studied for thrust vector control of ion thruster arrays.

D. Space Experience of Ion Thrusters

In August 1958 the first ion thruster experiments were conducted. On July 20, 1964 the SERT I spacecraft was launched. A four-stage Scout followed a ballistic trajectory over the Atlantic Ocean, providing two ion thrusters 47 min of space environment. One of the two

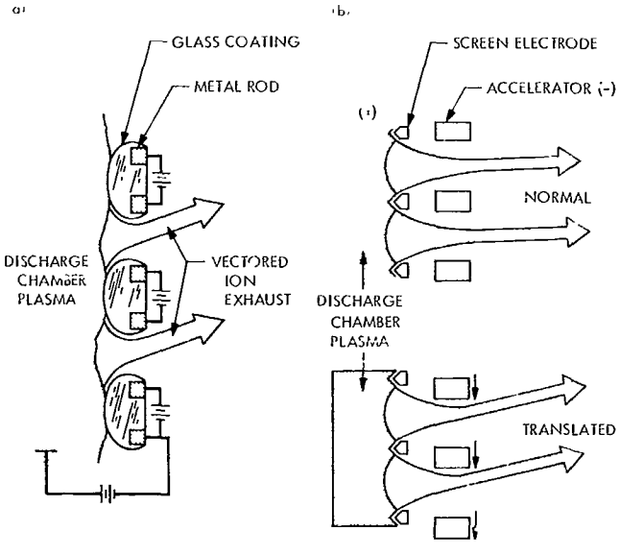

Fig. 9. Electron-bombardment thruster: (a) electrostatic beam deflection, and (b) accelerator grid translation

thrusters, a cesium contact-ion thruster, was unable to operate due to a high-voltage short circuit. The other, a mercury-bombardment thruster, successfully operated for over 31 min. Three flights of the Blue Scout vehicle were used to place cesium contact thrusters (EOS) into ballistic trajectory. The second flight was successful and data on the cesium contact-ionization thruster were returned. An EOS cesium contact-ion thruster was launched onboard Snapshot satellite; operation of its engine was unsuccessful. More recently a cesium contact thruster was flown on ATS-D and operated successfully. The SERT II was orbited on February 3, 1970. Data on the two mercury-bombardment thrusters on this satellite have been returned. One of the two thrusters failed after more than 3800 h of operation; at this point the second thruster was made operational. The second thruster failed after 2000 h. Failure of both thrusters has been identified as a result of impingement of neutralizer generated particles on the accelerator electrode.

E. EOS ATS-D and -E Contact-Ion Microthruster

Electro-Optical Systems has designed several contact-ion microthruster systems. The most recent thruster design is the 0- to 89-μN (0- to 20-μlbf) cesium contact-ion microthruster system developed for the ATS-D and -E satellites (Refs. 13 and 14). The thruster employs a single-button porous-tungsten ionizer. The thruster system is complete with propellant feed system, power conditioning, and 12 telemetry channels. Thrust vectoring ($\pm$ 10 deg) is accomplished by electrostatic beam deflection. A tantalum (50 ppm yttrium) hot-wire neutralizer is employed. Two neutralizers are provided; one is a backup in case of failure of the active neutralizer. The complete thruster system is depicted in Fig. 10.

The cesium propellant is stored in a cylindrical reservoir enclosing a fin array. There are 120 fins with spacing of 0.16 cm (0.064 in.) at the outer edge of the array. Cesium is fed to the center of the array where a porous nickel rod carries cesium through a sheathed vaporizer heater (0 to 4 W are required for vaporization of cesium). Propellant is sealed in the propellant tank assembly with an Invar tube with a nickel tip, which seats into an aperture in the vapor feed line. During vaporizer and ionizer operation, the feed line is automatically opened because of the difference in thermal expansion between the Invar tube and its stainless steel housing. The power conditioning efficiency is 60%. Three high voltages are required: beam voltage (+3000 V), deflection voltage, and accelerator voltage (−2000 V), along with low-voltage power to the ionizer, vaporizer, and neutralizer. The complete system, including power conditioning, propellant feed system, and thruster, has a mass less than 2.7 kg (6 lbm).

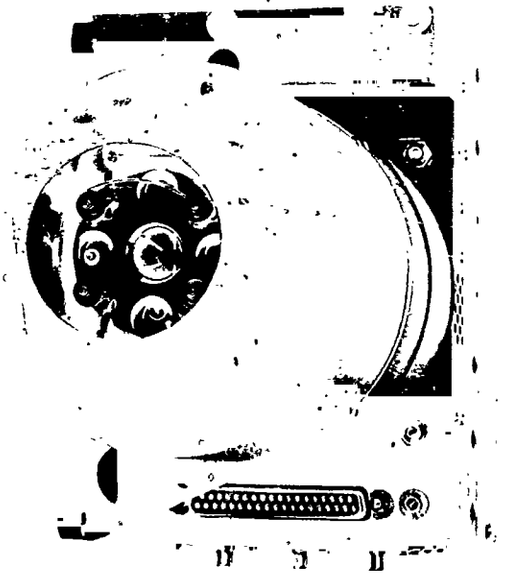

Fig. 10. EOS ATS-D and -E contact-ion microthruster (photo courtesy of EOS)

The system is capable of thrust level selection with nominal preset points of 0-, 22-, 44-, 67-, and 89-μN (0-, 5-, 10-, 15-, and 20-μlbf) thrust. Operation at 89-μN (20-μlbf) thrust has led to problems; the system operates best below this value. Typical operating data are presented in Table 1 (Ref. 13). These data were taken from flight acceptance testing where the thruster operated for 12 h in vacuum at 5 to 30°C with three on-off cycles.

The ionizer requires a constant 9.7 W to maintain the porous tungsten button at approximately 1040°C. The tantalum neutralizer requires a fixed 3.5 W. The electrostatic beam deflection system uses an insignificant amount of power.

Life testing of two ATS-D and -E contact-ion thrusters can be used as an indicator of thruster expected life (Ref. 15). Program goal was 3000 h of steady state operation at 67-μN (15-μlbf) thrust. One unit accumulated 2245 h of operation at 67 μN (15 μlbf) during a total test time of 3481 h; however, high accelerator current drain conditions led to the decision to terminate the test. An investigation of the drains was undertaken. Sputterback from the test chamber walls was the suspected cause of accelerator current drain. The conclusion yields no prediction of how long the thruster is expected to operate in a space environment where sputterback is not a problem. Test data returned from the ATS-D satellite indicate low accelerator current drain during the satellite's brief (less than 10 h) testing periods (Ref. 14). From these data, thruster lifetime (space environment) of 3000 to 5000 h can be expected without large accelerator electric current drains.

Extended life tests of tantalum and tantalum (50 ppm yttrium) neutralizer filaments were conducted. Four tantalum-yttrium filaments operated in excess of 10,000 h, while two pure tantalum filaments failed at less than 10,000 h. All six were tested at a pressure of 8×10^{-6} N/m^2 or lower, to avoid hydrocarbon vapors that could embrittle the filaments. The neutralizer performed well during the tests of the ATS-D experiment, except at one point (spacecraft potential was −132 V) when the demand for neutral current was so great that the neutralizer was emission limited. Spacecraft potential was measured in the fifth test (Ref. 14) of the experimental contact-ion thruster on ATS-D. A sudden dip in spacecraft potential (−42 to −132 V) was recorded. The dip in spacecraft potential was the result of one of the gravity-gradient booms passing through the ion thruster exhaust beam.

F. Hughes Research Laboratories Contact-Ion Microthruster

Hughes Research Laboratories (HRL) has developed a cesium contact (button type) thruster (Refs. 16 and 17). The thrust level can be selected from 0 to 89 μN (0 to 20 μlbf). The thruster employs a single button porous tungsten ionizer. The thruster system is complete with feed system, power conditioning and telemetry circuits. Thrust vectoring ($\pm$11°) is accomplished by electrostatic beam deflection. A thoriated-tungsten thermionic emission neutralizer is employed. Two neutralizers (two wires per neutralizer) are provided, one is a backup in case of failure of the active neutralizer. The complete thruster system is depicted in Fig. 11.

Cesium propellant is stored in a porous metal sponge made of Feltmetal.[2] Channels have been included to allow for the expansion of pressurant gas. A cylindrical propellant tank surrounds the Feltmetal sponge. Cesium is fed by capillary action through a porous nickel wick to the vaporizer. Cesium propellant is sealed in the storage tank by a bimetal valve to provide vacuum seal during storage, and shut off cesium vapor flow in the event of an unexpected power failure.

The thruster has a mass of 3.4 kg (7.51 lbm) with a maximum propellant capacity of 0.06 kg (0.13 lbm). The power conditioner provides beam (0 to +3000 V), accelerator (0 to −2500 V), and deflector (0 to −1000 V) high voltages along with ionizer, vaporizer and neutralizer power. The power conditioner operates at 70% efficiency and has a mass of 2.3 kg (5.0 lbm). The complete system has a mass less than 5.9 kg (13 lbm). This thruster is capable of 0- to 89-μN (0- to 20-μlbf) thrust with typical performance data presented in Table 1 (Ref. 17). An ionizer power of 12 W maintains the porous tungsten ionizer at 1350°K. The thoriated-tungsten wire neutralizer requires a fixed 1.8 W power.

Predicted life of this thruster is based on previous accelerator electrode erosion calculations presented in Fig. 12. At 89-μN (20-μlbf) thrust or 8-mA/cm^2 current density the accelerator electrode has two years of steady-state life. Accelerator electrode erosion predictions do not address the accelerator current drain problem, which terminated the life test of the EOS microthruster, and may well be the main factor affecting thruster life.

[2]Trademark of Huyok Corporation.

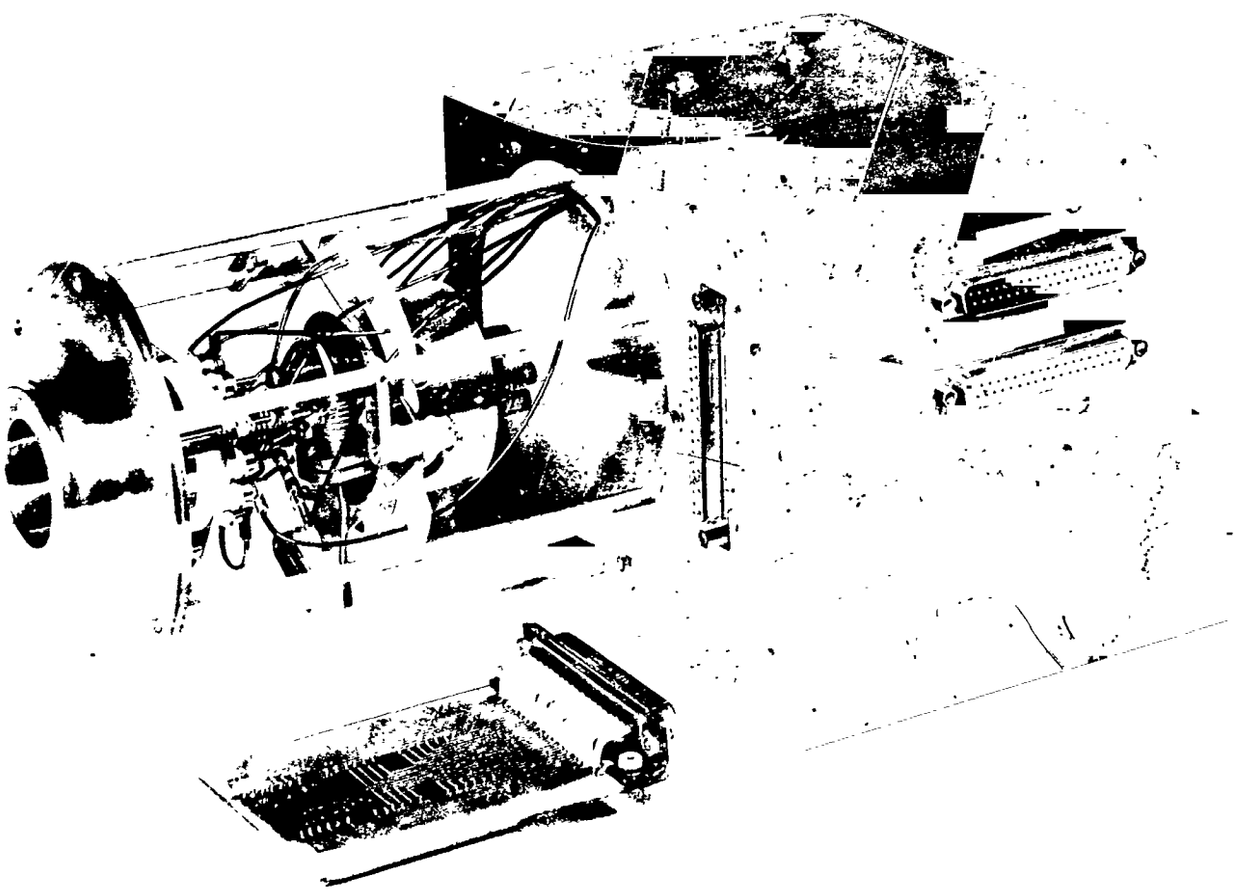

Fig. 11. HRL contact-ion microthruster (photo courtesy of HRL)

Table 1. Ion thruster performance data

Thruster type	Thrust, μN (μlbf)	Thruster power, W	Specific impulse, N-s/kg (lbf-s/lbm)	Power/thrust, W/mN (W/mlbf)	Mass utilization efficiency, %	Engine efficiency, %	Power conditioning efficiency, %	Total power, W
EOS ATS-D and -E cesium contact-ion microthruster	22 (5)	15.0	76,982 (7850)	1290 (5510)	~100	5.7	54.3	27.6
	44 (10)	16.6	103,950 (10,600)	671 (2980)	~100	13.9	55.7	29.8
	67 (15)	18.1	70,118 (7150)	455 (2020)	~100	12.9	58.9	30.7
	89 (20)	26.0	65,705 (6700)	369 (1640)	~100	14.6	61.7	32.4
HRL cesium contact-ion microthruster	22 (5)	21.0	65,705 (6700)	946 (4200)	~100	3.5	67.0	32.0
	44 (10)	23.0	65,705 (6700)	523 (2300)	~100	6.4	69.0	33.0
	67 (15)	27.0	65,705 (6700)	405 (1800)	~100	8.1	71.0	38.0
	89 (20)	28.0	65,705 (6700)	315 (1400)	~100	10.4	72.0	39.0
HRL 2.7 mN (600 μlbf) cesium linear-strip contact-ion-thruster	2669 (600)	167.0	49,033 (5000)	63 (280)	~100	39.0	85.0	196.0
	2669 (600)	190.0[a]	49,033 (5000)	71 (316)[a]	~100	34.0	85.0	224.5
EOS 450 μN (100 μlbf) cesium electron-bombardment thruster	453 (102)	31.7	38,344 (3910)	70 (310)	69.9	27.5	74.5	42.5
EOS 4.5 mN (1 mlbf) cesium-bombardment thruster	4.53 (1.02)	117.0	23,732 (2420)	26 (115)	90.0	46.0	83.0	141.0
HRL 5-cm mercury-bombardment thruster	1643 (370)	54.5	18,829 (1920)	32 (140)	75.0	26.2	85.0	64.0

[a]Includes power increases for dirty ionizer, and power increases for tungsten neutralizer.

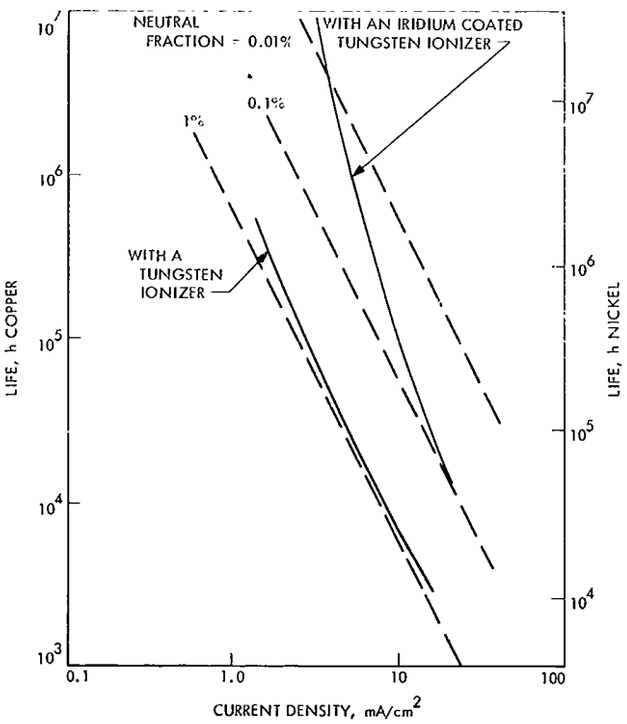

Fig. 12. Erosion of the accelerator electrode due to charge exchange ion bombardment (Ref. 19)

G. HRL Dual Beam Linear Strip Contact-Ion Thruster

Hughes Research Laboratories (HRL) has developed several long-life strip cesium contact-ion thrusters covering the thrust range of 0.44 to 4.4 mN (0.1 mlbf to 1.0 mlbf) (Refs. 18 and 19). The thruster employs a linear-strip, porous-tungsten ionizer. An orthogonal set of two thrusters (each 4.6 cm in length) is presently being developed into a thruster system with two zero-gravity, cesium-feed systems. The feed systems are similar to those developed for the HRL cesium microthruster. Thrust vectoring (±20°) is accomplished by electrostatic beam deflection. The thruster has been developed complete with a thoriated-tungsten thermionic neutralizer. Power conditioning efficiency and mass must be estimated, because the development thruster system will use breadboard power conditioning. The complete thruster system is depicted in Fig. 13.

The feed systems (each strip has its own) are identical to those described in the HRL microthruster system, except that the capacity of each tank has been enlarged to 0.07 kg (0.155 lbm) of propellant. The two reservoir assemblies have a mass of 1.0 kg (2.2 lbm) empty. The thruster has a mass of 1.4 kg (3.1 lbm) resulting in a total thruster system mass of 2.4 kg (5.3 lbm) with empty tanks. The power conditioning mass for this system has been estimated[3] at 5.5 kg (12 lbm), and a power conditioning efficiency of 85% can be assumed.

A 4.6 cm linear strip ion thruster operates at 1330-mN (300-mlbf) thrust with a 49,000-N-s/kg (5000-lbf-s/lbm) specific impulse. A pair of orthogonal 4.6 cm thrusters develops 2.7-mN (600-μlbf) thrust. Typical performance data are presented in Table 1.[4] A power of 38 W is required for each strip ionizer. In a degraded mode (dirty ionizer), the ionizer power requirement can be as high as 59 W. An estimated power of 2.6 W is required for each carburized-thoriated-tungsten neutralizer. A conventional tungsten neutralizer would require as much as 5 W for a 16.5 mA emission current. A power of 3 W

[3]H. J. King, HRL, personal communication, July 1970.

[4]C. Dulgeroff, HRL, personal communication, Nov. 1970.

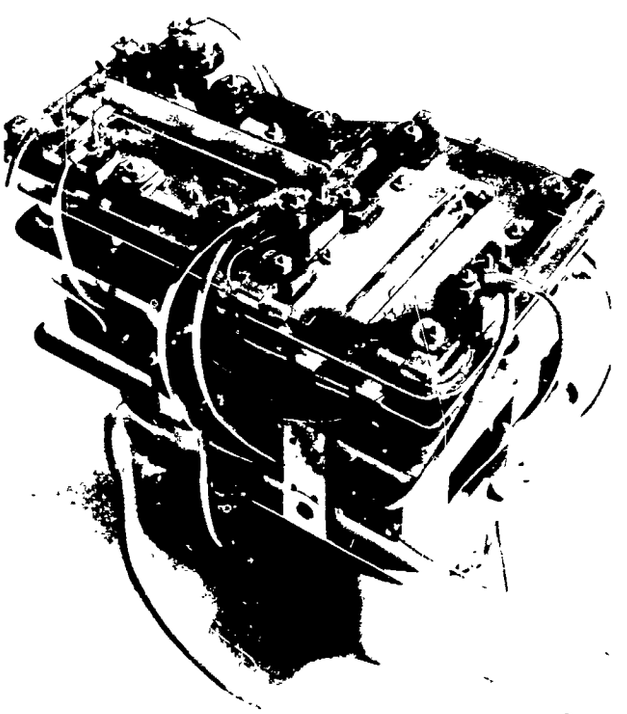

Fig. 13. HRL dual beam linear strip contact-ion thruster (photo courtesy of HRL)

is required for the propellant tank vent valve; however, valve actuation is a one time process.

Life tests of an 8-cm single strip ion thruster have been performed (Refs. 18 and 19). After 2000 h of steady-state operation the thruster still performed well. Measurements of accelerator erosion were taken and an estimation of its lifetime because of erosion was calculated. The rate of accelerator electrode erosion was extrapolated linearly as in Fig. 12. At a current density of 7 mA/cm^2, accelerator lifetime is estimated to be 14,000 h or 1.6 years. Accelerator drain current rose during the test, indicating that thruster performance was decreasing. In the HRL linear strip ion thruster life test, high accelerator drain currents were believed to be caused by the backsputtering from the vacuum test chamber. Backsputtering in a test chamber environment is greater than would be experienced in space. Again, estimation of accelerator current drains in space is difficult.

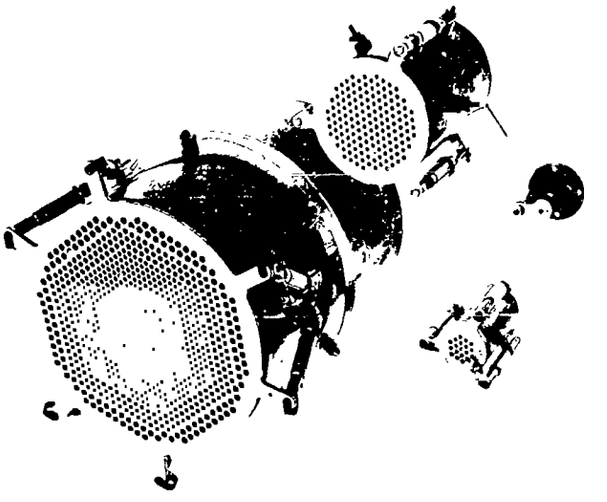

Fig. 14. EOS cesium bombardment thrusters (photo courtesy of EOS)

H. EOS 444-μN (100-μlbf) Cesium Bombardment Thruster

A great number of electron-bombardment thrusters have been fabricated and tested. Cesium-bombardment ion thrusters have been under investigation at EOS for several years. Early studies (Ref. 20) were directed toward characterization of cesium electron-bombardment thrusters over a wide thrust range. As a result of these early studies, a flight-prototype 444-μN (100-μlbf) cesium bombardment thruster system was developed (Refs. 21 and 22). The system includes an ion engine, zero-g feed system, neutralizer, and power conditioning. Thrust vectoring ($\pm 9°$) is accomplished by accelerator grid translation. A plasma-bridge neutralizer is incorporated in this system. The 444-μN (100-μlbf) thrust cesium-bombardment thruster is depicted in Fig. 14 (19 holes in grid) along with several other cesium bombardment thrusters.

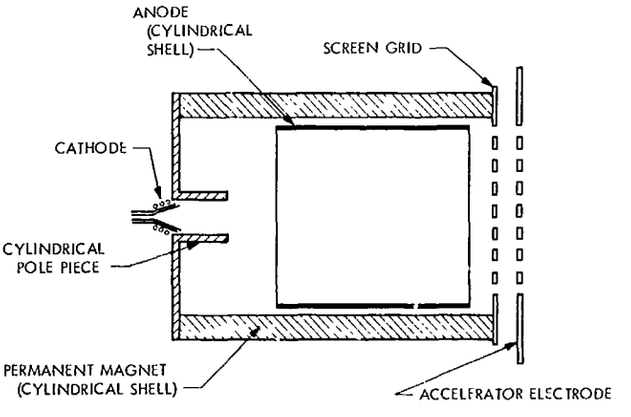

Fig. 15. EOS 445-μN (100-μlbf) cesium electron-bombardment thruster discharge chamber

The 444-μN (100-μlbf) cesium-bombardment thruster utilizes a cesiated tantalum cathode for long life, and permanent magnets for low discharge chamber power. A magnetic pole piece is also incorporated in the discharge chamber (Fig 15) to intensify the cathode permanent-magnet flux density. Accelerator displacement is used as a means of thrust vectoring (see Fig. 9b). Thermal expansion forces are used to displace the accelerator perpendicular to the engine axis creating $\pm 9°$ of thrust vectoring. Cesium propellant is stored in a cylindrical reservoir enclosing a fin array. There are two tanks, one for the thruster cathode and the other for the plasma-bridge neutralizer. Each tank employs capillary forces to draw cesium propellant to a porous-nickel rod that feeds propellant to the vaporizer. Each tank is evacuated for launch and sealed with cadmium plugs (the plugs evaporate when heated). A plasma-bridge, or discharge neutralizer, was chosen for its excellent beam coupling and long-life characteristics. The neutralizer is a small cathode (500°C) that emits electrons and cesium ions. A plasma bridge between the neutralizer cathode and exhaust ion beam is formed, resulting in ion beam potentials of about 10 to 20 V with the neutralizer about 2.5 cm (1 inch) from the edge of the ion beam. The neutralizer requires approximately 5 W and consumes 6.8 mg of cesium per hour of operation. The power

conditioning efficiency is 74% for this system. The power conditioning system provides high voltages for the accelerator grid and the beam, along with power-to-grid displacement heaters, vaporizers, cathode, neutralizer, and a preheater. The complete thruster system mass, including power conditioning, propellant feed system, and thruster, is below 2.3 kg (5 lbm). Included in this mass is 0.7 kg (1.5 lbm) of thruster propellant and 0.05 kg (0.1 lbm) of neutralizer propellant.

The cesium electron-bombardment thruster develops a nominal 457-μN (103-μlbf) thrust at 45,100-N-s/kg (4600-lbf-s/lbm) specific impulse with a discharge chamber mass efficiency of 83%. Because the thruster employs a plasma-bridge neutralizer, a slight adjustment in thruster specific impulse and mass efficiency must be made to account for the unaccelerated cesium propellant expelled from the plasma-bridge neutralizer. This is reflected in a total system mass efficiency (percent unaccelerated propellant) of 69.9%. Detailed thruster system performance data are presented in Table 1 (Ref. 21). The neutralizer required 5 W to maintain the device at 500°C. Deflection of the accelerator grid requires less than 1 W.

System integration tests were performed with a complete thruster system. All of the system components performed at their specified levels. No adverse component interactions were found. Life testing of this system was not performed; however, earlier studies at EOS (Ref. 23) with cesium electron-bombardment thrusters included several life tests of thruster systems. Life tests of a 28.9-mN (6.5-mlbf) cesium electron-bombardment thruster for more than 8,000 h indicate long life of cesium-bombardment thruster grids. A life of 20,000 h was predicted from the measurement of accelerator grid erosion. The plasma-bridge neutralizer failed after 8,100 h of test, because of clogging of the neutralizer propellant orifice. Backsputtered material from the test chamber walls was blamed for neutralizer clogging, and operation in a space environment should alleviate this mode of neutralizer failure.

I. EOS 4.44-mN (1.0-mlbf) Cesium Bombardment Thruster

Electro-Optical Systems has recently developed a 4.44-mN (1.0-mlbf) thrust cesium-bombardment ion thruster for north-south stationkeeping on the synchronous ATS-F satellite (Ref. 24). The system includes an ion engine, zero-g feed system, neutralizer, and power conditioning. Thrust vectoring (±7°) is accomplished by accelerator grid translation. The ion engine employs

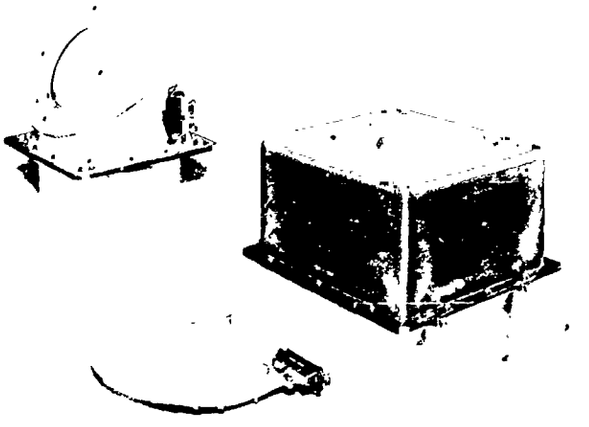

Fig. 16. EOS 4.45-mN (1-mlbf) cesium bombardment thruster (photo courtesy of EOS)

the highly efficient magnetoelectrostatic containment (MESC) discharge chamber and a plasma-bridge neutralizer. The 4.44-mN (1.0-mlbf) cesium electron-bombardment thruster system is depicted in Fig. 16.

The thruster employs magnetoelectrostatic plasma containment (see Fig. 6 and Ref. 25). Bounding surfaces of the discharge chamber act as a magnetic wall to reflect most of the ions and electrons approaching them. This greatly reduces ion losses to the walls, increases mass utilization efficiency, and provides a uniform plasma for efficient ion extraction. Ten percent of the propellant flows through a hollow cathode (~500°C) which acts like an autocathode after discharge power (~3W) is initiated. The remainder (90%) of the cesium propellant is introduced to the discharge chamber through a feed ring biased at the potential of the boundary anodes. Thrust vectoring and feed systems are similar to those in the 444-μN (100-μlbf) EOS cesium electron-bombardment system, except three feed systems are required for the MESC thruster, one for the plasma-bridge neutralizer, one for the thruster cathode, and one for the thruster anode. Each feed system is sealed with a thermally actuated bimetal valve similar to that used on the ATS-D contact-ion microthruster. Capacity of the feed systems can be increased or decreased with the ATS-F feed system storing 3.4 kg (7.4 lbm) of cesium (0.64 kg or 1.4 lbm for the cathode) for the discharge chamber and 0.09 kg (0.2 lbm) for the plasma-bridge neutralizer. Feed system container mass is 2.0 kg (4.5 lbm). The plasma-bridge neutralizer requires approximately 8 W power

and consumes 24 mg of cesium per hour of operation. The power conditioning efficiency is 83% for this system, which provides high voltage to the discharge chamber and accelerator grid along with power to grid displacement heaters, vaporizers, cathode, and neutralizer. Power conditioning system mass was 8.6 kg (19 lbm), with a total system mass of 15 kg (33 lbm). These mass data include 3.5 kg (7.6 lbm) of cesium.

The MESC electron-bombardment thruster develops a nominal 4.57-mN (1.03-mlbf) thrust at 24,500-N-s/kg (2500-lbf-s/lbm) specific impulse with a discharge chamber mass efficiency of 93%. These data must be adjusted to account for the unaccelerated cesium propellant expelled from the plasma-bridge neutralizer. This results in a system specific impulse of 23,700 N-s/kg (2420 lbf-s/lbm) and a 90% mass efficiency (percent unaccelerated propellant). Detailed thruster system performance data taken from a 465-h integration test are presented in Table 1 (Ref. 24). The neutralizer required 5 to 11 W.

The system has undergone 465 h of test with successful system operation. No lifetime data of the MESC thruster are presently available; however, the early life tests of cesium electron-bombardment thrusters discussed previously herein are again applicable for predictions of thruster life.

J. Five-Cm Mercury Bombardment Thruster

Low-thrust mercury-bombardment thruster research has been underway at NASA Lewis Research Center (LeRC) for several years. The most recent low-thrust mercury electron-bombardment thruster (Refs. 26 and 27) employs a 5-cm-diameter discharge chamber and a glass-coated grid. A series of preliminary thruster tests was conducted at LeRC with a variable-geometry discharge chamber. Hughes Research Laboratories are presently developing this experimental thruster into a flight-prototype system capable of providing north-south stationkeeping of a synchronous satellite. The system includes ion engine, zero-g feed system, and neutralizer. Thrust vectoring (±10 deg) is accomplished by electrostatic beam deflection. The ion engine utilizes a plasma-bridge neutralizer. The LeRC 5-cm mercury electron-bombardment thruster system is depicted in Fig. 17.

The thruster employs a 5-cm-diameter permanent magnet discharge chamber (Fig. 18). A hollow enclosed cathode and a conical cathode pole piece are used to improve discharge chamber performance at the low thrust. Glass-coated grids are incorporated to reduce discharge power losses at low specific impulses. All the propellant flow goes through the hollow enclosed cathode. The method of thrust vectoring is not firmly established; however, an electrostatic thrust vectoring scheme is being extensively investigated at HRL. Glass grids capable of electrostatic beam vectoring are not presently developed; however, experimental two-grid systems have demonstrated the technique.[5] The 5-cm mercury-bombardment thruster could rely on a standard glass grid and engine gimbaling, or a two-grid system and grid translation to provide thrust vector control. The

[5]H. J. King, HRL, personal communication, Jan. 1971.

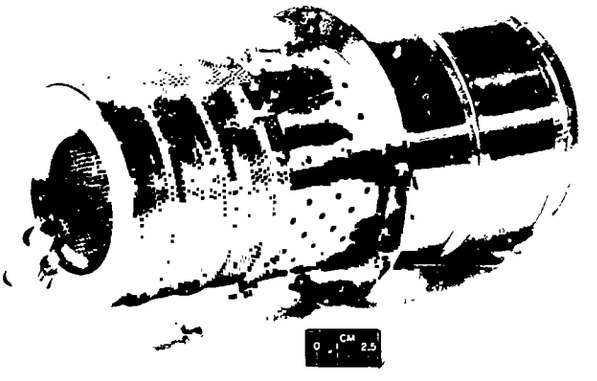

Fig. 17. Five-cm mercury bombardment thruster (photo courtesy of LeRC)

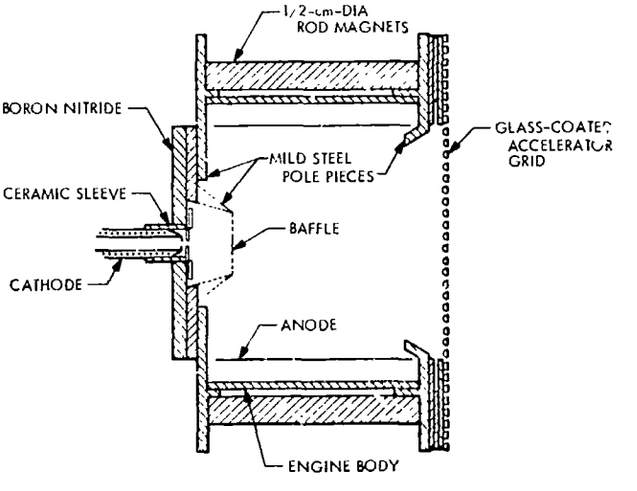

Fig. 18. Five-cm mercury bombardment thruster discharge chamber (representative of HRL and LeRC designs)

feed system is similar to the SERT-II mercury feed system. The propellant is stored in a reservoir and expelled by a pressurant gas. An elastomeric bladder is used for propellant-pressurant separation. The feed system of the design has a mass of 1.0 kg (2.2 lbm) and a capacity for up to 6.2 kg (13.6 lbm) of mercury. An isolator is provided so that the main cathode and the neutralizer can share the same propellant tank. The plasma-bridge neutralizer is designed to provide sufficient electrons to neutralize a 30-mA beam with 6.3% of the main propellant flow required for the neutralizer. A power conditioning system mass of 2.7 kg (6.0 lbm) is estimated,[6] with an efficiency of 85% expected. The total system has an estimated mass of 2.3 kg (5.1 lbm) with a maximum propellant capacity of 6.2 kg (13.6 lbm) of mercury.

The HRL 5-cm mercury-bombardment thruster develops 1640-μN (370-μlbf) thrust at a nominal 18,800-N-s/kg (1920-lbf-s/lbm) specific impulse with a discharge chamber mass efficiency of 75%. Discharge chamber mass efficiency includes neutralizer propellant consumption. Detailed thruster performance data taken from Ref 27 are presented in Table 1. The plasma-bridge neutralizer requires a maximum of 12.0 W.

Life test data of this thruster system are not available because it is still in the developmental stage. Grid lifetime seems to limit thruster life at present. During a 1000-h life test of a 15-cm glass-coated grid, (Ref. 28), weight loss measurements indicated that the grid would be 100% eroded in 22,000 h. This life test was divided into two parts: 500 h of normal operation followed by 500 h of grid-edge-termination studies. During the second 500 h of testing, this grid was modified with masks over the edges of the grid. Although lifetimes of 10,000 h have been projected for glass-coated grids, a great number of glass grids have failed after a few hours of test. Long-lived glass grids seem to depend heavily on extremely tight quality control, since irregularities in glass coating induce premature failure, (Ref. 28). It has also been speculated that interactions with the test facility may be responsible for such failures, making ground test of these devices very difficult (Ref. 29).

Two-grid bombardment thrusters (these operate at a somewhat higher voltage or specific impulse than glass-coated grid thrusters) have undergone extensive life testing. The 15-cm SERT-II mercury-bombardment thruster has been life-tested at several facilities. Thruster tests have exceeded 5000 h; however, excessive erosion near the neutralizer was noted. In a space test of the thrusters, one system operated for more than 3,800 h before failure, while a second thruster operated successfully for more than 2,000 h. Failure of the thrusters has been identified as a result of extensive grid erosion near the neutralizer. Proper design and placement of the neutralizer should alleviate this problem in future thrusters. In earlier studies of mercury-bombardment thruster lifetime, grid erosion rates were estimated (Ref. 30). Lifetimes of 10,000 h for a 20-cm mercury-bombardment thruster were estimated on the basis of observed grid erosion rates.

Sputter yield (i.e., number of metal atoms eroded per incident ion) is an increasing function of ion energy or the potential difference between the accelerator grid and neutralizer. Therefore, increased grid life can be expected for the 5-cm mercury-bombardment thruster because the negative accelerator voltage (−250 V) is nearer spacecraft potential than the SERT-II negative accelerator voltage (−1750 V). Accelerator grid erosion is also a function of current density; however, the SERT-II and the 5-cm thruster are of comparable current density. The two-grid, 5-cm mercury-bombardment thruster with proper neutralizer geometry should provide 10,000 h of life.

Plasma-bridge neutralizers have been tested in conjunction with thruster life tests. One mercury-bombardment thruster test was in excess of 5000 h. An endurance test of a SERT-II (Ref. 31) design neutralizer has been conducted. The plasma-bridge neutralizer operated for 12,000 h, emitting 250 mA to a collector plate.

III. Colloid Thrusters

A. What Is a Colloid Thruster?

The colloid thruster is defined as a device that electrostatically accelerates multi-atom or multi-molecular charged particles. Solid and liquid heavy particles have been studied; however, liquid colloids have proved most successful. A conceptual diagram of a colloid thruster is presented in Fig. 19. Liquid propellant (glyceral to which sodium iodide is added) is stored in a reservoir, which can be a rigid tank, a coiled feed tube, or a bellows tank. If the propellant is pneumatically fed as in the system presented in Fig. 8, then a propellant isolation

[6]H. J. King, HRL, personal communication, July 1970.

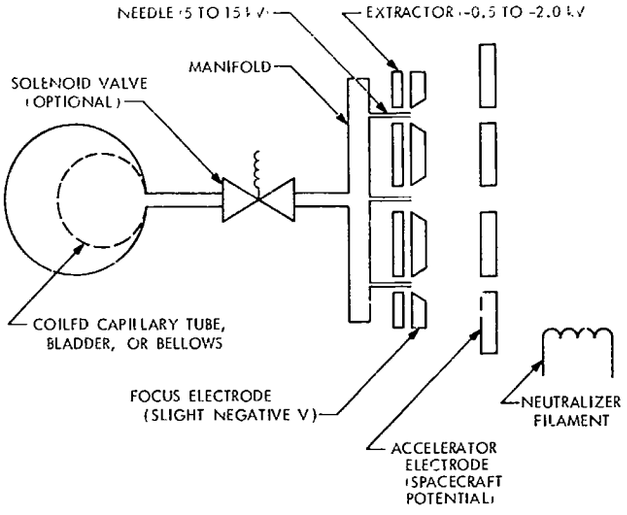

Fig. 19. Conceptual diagram of a colloid thruster

valve is required. If a bellows is used, then the propellant can be fed mechanically, and therefore an isolation valve is required only to protect the propellant from an atmosphere prior to launch. The propellant is distributed in a manifold to needles, linear slits, or annular slits (Fig. 20). A potential is maintained between the needle and the extractor electrode. The intense electric field in the vicinity of the thin needle rim exerts a force upon the fluid surface, producing electrohydrodynamic spraying of charged propellant droplets. These multi-molecular droplets are charged positive when the capillary is maintained at a positive potential and negative when the voltage potential is reversed. A focus electrode is required to contain the charged droplets within the accelerator gap. The accelerator electrode is maintained at spacecraft potential. In recent thrusters, the focus and accelerator electrodes have been removed. Again as in the ion thrusters, a neutralizer is required; however, the lower charge/mass ratio for colloid systems as compared to ion thruster systems dictates substantially lower neutralizer requirements for a colloid thruster of comparable thrust.

3. History of Colloid Thrusters

The early studies in electrostatic thruster technology were not devoted solely to the acceleration of charged ions. Indeed, the acceleration of charged colloidal particles was the subject of an early paper by H. Preston-Thomas (Ref. 32).

During the very active period of 1957-58, studies on colloid propulsion were initiated at Aerojet-General (Ref. 33) and Thiokol Chemical Corporation (Ref. 34). Early work was centered around solid colloid particles; however, later work utilized liquid colloid droplets.

Studies by R. Hunter at Air Force Aero Propulsion Laboratory (AFAPL) were initiated in 1959 (Ref. 35). This work developed into studies at the University of Illinois with C. Hendricks (Ref. 36) and with TRW Systems (Ref. 37). Work at TRW, ultimately under E. Cohen, resulted in a heavy charged particle thruster for space propulsion (Ref. 38). Other colloid research (bipolar operation and propellant evaluations) continued at AFAPL (Ref. 39) and NASA LeRC (Ref. 40).

Electro-Optical Systems developed a 73-needle bipolar thruster in 1967 (Ref. 41) and by 1968 a colloid microthruster system was developed by TRW Systems (Ref. 42).

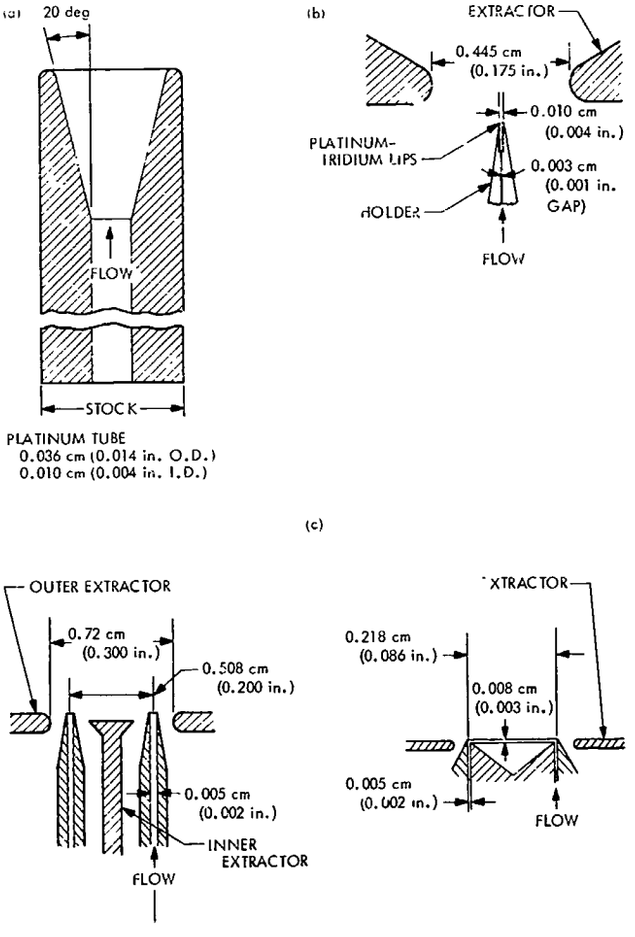

Fig. 20. Geometry of needles and slits: (a) standard needles, (b) linear slits, and (c) annular slits

C. Characteristics of Colloid Thrusters

Propellant evaluation programs have led to the conclusion that glycerol doped with sodium iodide is the best propellant. Colloid thrusters presently under development employ this propellant almost exclusively. The superior performance of glycerol is due to its unique combination of properties:

(1) High dielectric constant, which allows glycerol doped with ionic salts to form a conducting solution.

(2) Low vapor pressure, which minimizes evaporation at needle tips.

(3) High viscosity, which provides very low mass flow rates compatible with rates of electrohydrodynamic spraying.

Needles have been used in most colloid thruster studies. A typical needle is presented in Fig. 20. The needle material is usually platinum-10% iridium; however, pure platinum and platinum-20% iridium have also been employed. Each needle develops 8.9- to 40-μN (2- to 9-μlbf) thrust, with operation at 8.9 to 13.3 μN (2 to 3 μlbf) desired for long life. Thrust levels are attained by using multi-needle modular arrays.

Experimental studies using annular and linear slits rather than needles are being conducted. Typical linear and annular slit geometries are presented in Fig. 20. Recently, most experiments have dealt with annular slits, because these indicate longer possible lifetimes than linear slits.

One major advantage of the colloid system for auxiliary electric propulsion is its specific impulse resulting from the large charge-to-mass ratio of colloid particles. A colloid thruster operating at the same mass utilization efficiency and net accelerating voltage as an ion engine will have a lower specific impulse, because specific impulse is proportional to the square root of the charge-to-mass ratio. The colloid will operate well around 14,710 N-s/kg (1500 lbf-s/lbm), with a somewhat larger net accelerating voltage than typical ion thrusters. Although the colloid thruster requires more propellant than an ion thruster, the greater mass penalty for the power of an ion thruster results in a lower total system mass for the colloid thruster. Therefore, the colloid specific impulse is more attractive for missions with total impulse requirements below 17,760 N-s (40,000 lbf-s) than the higher ion-thruster specific impulse of 24,420 N-s/kg (3000 lbf-s/lbm).

Electrostatically accelerated thruster systems require neutralizers; however, the beam current (a requirement for a neutralizer) for a colloid thruster is less than that produced by an ion thruster of equal thrust. The neutralizer requirements can be as much as 50 times lower for a colloid; therefore, thermionic neutralizers are practical (for thrust levels up to several millipounds).

The injection potential for a thermionic neutralizer is a strong function of the closeness of the beam to the neutralizer. The closer the two are coupled, however, the greater the erosion of the neutralizer. As a result, long-lived thermionic neutralizers must accept a moderate (20 to 50 V) injection potential. One method of eliminating the neutralizer requirement would be to emit positive and negative beams of equal magnitude (i.e., a bipolar operation). This scheme has been studied rather extensively, with several methods of implementation devised. Two implementations are presented in Fig. 21. The conventional approach (Ref. 43), (Fig. 21a) is to divide the thruster into two complete (feed system, needles, and accelerator) modules with one module negative and the other positive. Problems with gas evolution and thrust mismatch have led to the use of different propellants for the negative and positive modules. In an effort to reduce total system mass, an alternating pulse square wave generator (Ref. 44) can be employed (Fig. 21b). The voltage is pulsed on and off to side-by-side needle submodules of opposite polarity. Thus only one high voltage unit is required.

One disadvantage of the colloid system is its sensitivity to temperature; the viscosity of the propellant varies with temperature. The colloid will operate over a 0 to 40°C temperature range, but the thrust, flowrate, and accelerating voltages all vary widely within this range. Thermal control is therefore required to maintain the thruster at constant performance. The power requirement for thermal control of a colloid system on a synchronous satellite is low; however, power requirements on board a deep space spacecraft can be high. Also, the failure of the thermal control subsystem can lead to degraded thruster system operation and even failure of the system.

A disadvantage of the sodium iodide doped glycerol is its tendency to form particulate matter under electron bombardment; these particles clog the propellant needle tips. This problem is presently under study and seems to be one of the factors limiting colloid thruster life.

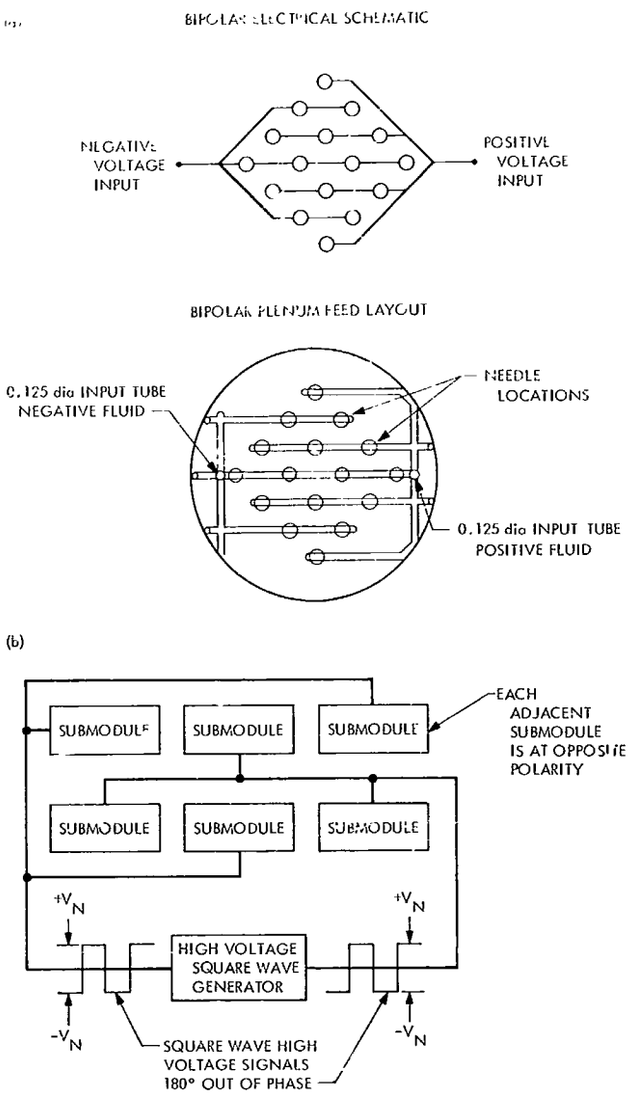

Fig. 21. Bipolar colloid arrays: (a) conventional array, and (b) block diagram of alternating pulse array

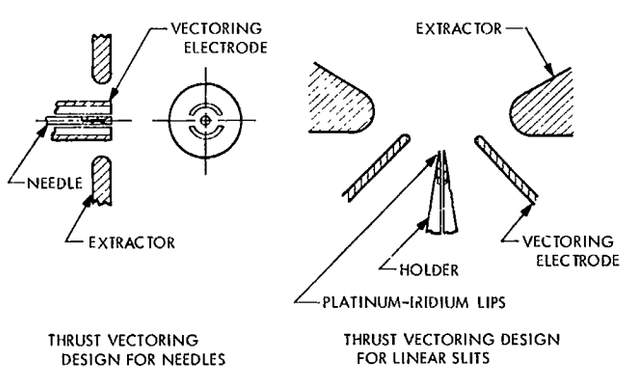

Fig. 22. Electrostatic beam deflection of colloid thrusters

Pulsing of a colloid thruster has been demonstrated. Electrostatic beam vectoring has also been demonstrated. A thrust vector design (Ref. 45) is presented in Fig. 22. By placing the vectoring electrodes of adjacent needles at right angles to each other, electrostatic beam vectoring within a 10° cone can be achieved.

D. Colloid Microthruster

To the time of this study there have been no orbital tests of colloid thrusters; however, TRW Systems Group has developed a colloid microthruster system (Refs. 42 and 46) consisting of a three-needle array thruster, neutralizer, zero-gravity propellant feed system, and power conditioning unit. This colloid system develops a nominal 36-μN (8-μlbf) thrust at 9320-N-s/kg (950-lbf-s/lbm) specific impulse and was originally developed for providing yaw control on a multipurpose satellite in synchronous orbit. When plans for the satellite were cancelled, the colloid thruster was redirected to laboratory testing. The complete prototype system is shown in Fig. 23.

Fig. 23. Colloid microthruster system (photo courtesy of TRW Systems Group)

The propellant, glycerol doped with sodium iodide, is stored in a coiled Inconel tube. The pressurant gas (argon) is contained in an annulus surrounding the propellant storage coils. The annulus gas volume is twice the initial propellant volume, so that feed pressure is reduced by 33%: 4800 to 3200 N/m² (36 to 24 torr) near complete expulsion. Propellant storage and expulsion tank mass is 0.8 kg (1.7 lbm) with 0.2 kg (0.5 lbm) of propellant. Because the propellant is constantly under pressure, an in-line propellant valve is required. Because of the very low propellant flow rates (e.g., 4 μg/s), a valve design that minimizes "pumping" of propellant through the capillary array during actuation is desired. A tungsten carbide ball seat is employed. Valve actuation is implemented with a thermal actuator (2 W). Dual valve assembly mass is 0.14 kg (0.3 lbm). The power conditioning unit must supply power to the propellant valve, neutralizer, and system heaters, along with high-voltage power to the propellant needles (4 to 8 kV) and the extractor electrode (400 to 800 V). With a nominal input of 5 W (spacecraft voltage) the unit can supply 1.4 W of conditioned power at a conversion efficiency of 28%. The mass of the power conditioning unit is 1.3 kg (2.9 lbm). A small thermal control heater is provided to maintain the thruster at a preset 25 or 30°C. Thruster mass is 0.05 kg (0.1 lbm) and structure mass is 0.7 kg (1.5 lbm). This results in a total system mass of 3.2 kg (7.0 lbm) including propellant.

Typical operating data are presented in Table 2. These data are for a 36-μA beam current and a thruster temperature of 29°C. Both the beam current and temperature remain fixed. Because the feed system operates from a blow-down propellant tank, the feed pressure decreases with propellant consumption. As feed pressure decreases, the mass flow rate of propellant decreases. The mechanism of electrohydrodynamic spraying is not well understood; however, at low mass flow rates particles are extracted at a somewhat larger average charge-to-mass ratio, which results in a decrease in thrust and an increase in specific impulse.

A life test of this thruster has been performed. Results from over 1750 h of microthruster operation are presented in Refs. 46 and 47. Thruster operation was good through 1300 h of log time[7] with a slight decrease in propellant mass flow rate. For a period of 70 h, a 0.3- to 0.5-μA extractor current persisted. The current leakage was finally corrected by operating the thruster with a closed valve and a high operating temperature. During the log hours period 1484 to 2348, a constant decrease in mass flow rate was noticed and thruster temperature was increased in attempts to improve the mass flow rates. Decreased mass flow rate was later explained by a leak in the pressurant gas tank. Another life test of the colloid microthruster is reported in Ref. 48. A three-needle array was tested for 1300 h when a power failure permitted the propellant to form a droplet between the needle and the extractor. A second test of the array lasted 2400 h with a similar power failure. At test termination, needle tips were in excellent condition; however, prevention of glycerol flow to the extractor and tar deposits due to electron bombardment of glycerol are necessary for long-life colloid thrusters.

In Refs. 46 and 47, the tungsten neutralizer was tested in conjunction with the thruster, and filament voltage was monitored during the test. A rapid increase in neutralizer voltage was noticed at 25 h into the test. This was attributed to carbiding of the tungsten filament due to the presence of hydrocarbons (colloid beam products) in the test chamber environment. A controlled oxygen leak was introduced to the chamber to counter the tungsten carbiding. Neutralizer operation was terminated after 950 h because of electron leakage to high voltage. The leakage was subsequently attributed to holes through the support insulators between the feed system and the thruster housing. Electron leakage was not evidenced after covering the support insulator holes during post test analysis.

E. TRW 4.4-mN (1-mlbf) Colloid ADP Thruster

A 4.4-mN (1-mlbf) thrust colloid system is presently under development at TRW Systems Group under sponsorship of the AFAPL.[8] The thruster will be comprised of twelve 36-needle modules. Each module will deliver approximately 355-μN (80-μlbf) thrust at a nominal 14,710-N-s/kg (1500-lbf-s/lbm) specific impulse. This system is designed for north-south stationkeeping of a synchronous satellite. A program goal is a 10,000-h thruster lifetime. An artist's conception of this thruster is depicted in Fig. 24.

[7]Time thruster was in vacuum.

[8]To be published as: Jackson, F. A., "Colloid Advanced Development Program," presented at the AFOSR Sixth Symposium on Advanced Propulsion Concepts, May 1971.

Table 2. Colloid thruster performance data

Thruster type	Geometry	Thrust, μN (μlbf)	Thruster power, W	Specific impulse, N-s/kg (lbf-s/lbm)	Mass flow rate, μg/s	Reference	Power/ thrust, W/mN (W/mlbf)	Engine efficiency, %	Power conditioning efficiency, %	Total power, W
TRW colloid micro-thruster[a]		39 (8.7)[b]	1.39[c]	9611 (960)	4.0	14	36 (160)	13.1	28.0	5.0
		23 (5.2)	1.43[c]	16,867 (1720)	1.5	14	70 (275)	13.6	29.0	5.0
		48 (10.8)	1.38[c]	7257 (740)	6.5	14	29 (128)	12.6	28.0	5.0
Typical colloid thrusters	36 needles	371.0 (83.5)	3.91	14,710 (1500)	24.9	Estimate	10.54 (46.8)	70.0		
	36 needles	383.0 (86.0)	3.80	14,691 (1498)	25.6	17	9.95 (44.2)	70.0		
	36 needles	306.0 (68.9)	3.30	14,318 (1460)	21.4	17	10.79 (47.9)	66.0		
	36 needles	345.0 (77.6)	3.80	14,837 (1513)	23.3	17	11.01 (48.9)	67.0		
	6 annular slits	534.0 (120.0)	5.54	15,200 (1550)	35.0	17	10.41 (46.2)	72.0		
	6 annular slits	512.0 (115.0)	5.52	14,906 (1520)	36.0	17	10.81 (48.0)	70.0		
	6 annular slits	489.0 (110.0)	5.22	14,514 (1480)	35.0	17	10.70 (47.5)	69.0		
	1 annular[d] slit (EOS)	89.0 (20.0)	0.87	13,141 (1340)	6.8	18	9.80 (43.5)	73.0		
TRW 4.5-mN (1-mlbf) ADP colloid	(footnote)[e]	4,450 (1000)	58.00[f]	14,710 (1500)	298.8	Estimate	13.0[f] (58)	56.0[f]	85.0	68.2

[a]Data at 29°C 36 ma.

[b]Design thrust level.

[c]Includes 0.82 W for neutralizer and 0.30 W for thruster heater.

[d]Data at 0°C.

[e]12 modules of 36 needles each with the performance of the fourth line of this table.

[f]Includes 5 W for neutralizer, 6 W for thruster heater and mass flow rate controller.

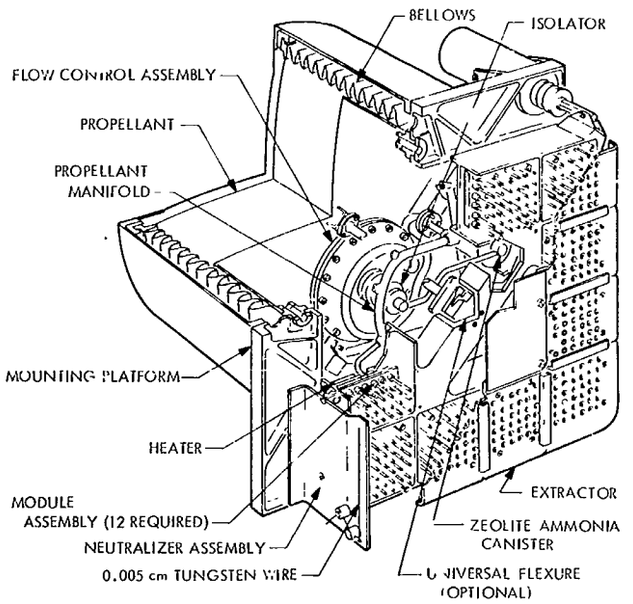

Fig. 24. TRW 4.45-mN (1-mlbf) colloid ADP thruster concept

The sodium iodide doped glycerol is stored in a bellows tank, with propellant flow rate mechanically controlled. Feed system mass is estimated at 2.9 kg (6.4 lbm) with a maximum propellant load of 11.3 kg (25 lbm). This allows for 10,000 h of thrusting at 14,710-N-s/kg (1500-lbf-s/lbm) specific impulse and a 95% mass expulsion efficiency. The mechanical flow controller operates on a feedback loop from the beam current. Average power requirement for the controller is 1 W with a maximum predicted peak power required of 2 W. The power conditioner must provide high voltages for the needles and extractor (up to 12.3 kV) along with power for the thruster heater, neutralizer, and propellant flow rate controller. The power conditioning subsystem is estimated at 3.1 kg (6.9 lbm) with a 85% efficiency. It will provide 70 W of conditioned power. Thruster mass is 0.95 kg (2.1 lbm) with a 2.0 kg (4.5 lbm) structural mass estimated. Total fixed system mass is 9.1 kg (20 lbm) with up to 11 kg (25 lbm) of propellant capacity.

Typical operating data for a 36-needle module is presented in Table 2. The fourth line corresponds to the design data used in estimating 4.4-mN (1-mlbf) thruster system performance. The following lines are test data obtained on several types of modules. The annular slit performance was taken from TRW Systems Group (Ref. 49) and EOS (Ref. 50) data. The final line in Table 2 is estimated performance of the 4.4-mN (1-mlbf) colloid thruster system. A heater power of 3.0 W is estimated for synchronous orbit of north-south stationkeeping thrusters. Neutralizer power is estimated at 5.0 W, providing 3.8 mA of negative current for 10,000 h.

Life test data are not available for a 4.4-mN (1-mlbf) thruster array. The life test of a 3-needle microthruster system has previously been discussed. Tests of 36-needle modules have exceeded 1000 h with little or no degradation in thruster performance (Ref. 49). Current leakage between the needle and extractor were noticed several times during the thruster life test. The vacuum pressure was increased, propellant feed pressure was lowered, and the beam was vectored in an effort to "clean up" the drainage currents. This was an effective solution; however, it is not the procedure that would be used in space. At 930 h the test was terminated when failure of vacuum equipment led to severe erosion of the thruster module. A six-annular-slit array was tested for 500 h. Tar formation was present and eventually led to termination of the test. New designs are being studied in an effort to eliminate long-term tar deposits in annular slits.

Neutralizers were tested in conjunction with the 1000-h 36-needle tests reported in Ref. 49. The neutralizer functioned properly for the first 180 h of the test when the chamber pressure was increased in an effort to "clean up" the thruster array. However, the neutralizer then burned up due to the presence of atmosphere.

IV. MPD Thrusters

A. What Is an MPD Thruster?

The magnetoplasmadynamic (MPD) arc thruster has evolved through experiments that incorporate arcjet technology and magnetogasdynamic channel flow. The arcjet utilizes a high-current-density discharge between a cathode and anode producing a hot gas that is expelled through a nozzle. The hot gas is ionized (i.e., plasma) and can therefore be accelerated electromagnetically. Magnetogasdynamic channel flow, sometimes referred to as magnetohydrodynamic acceleration (MHD), relies primarily on crossed field ($j \times B$) forces to accelerate a plasma. The MPD arc thruster combines an arc discharge with a crossed-field accelerator.

The MPD has been investigated primarily as a steady-state device; however, it may also be pulsed. Pulsed MPD thrusters with pulse lengths of 1 ms or greater are

referred to as quasi-steady-state MPD thrusters. The geometry of the quasi-steady-state MPD thruster does not differ greatly from that of a conventional steady-state MPD thruster.

A conceptual diagram of an MPD thruster is presented in Fig. 25. The primary components are the gas flow passages, the anode, the cathode, and the external field coil. Propellant, usually a gas, is fed from a storage tank through a valve (rapid pulse valve for quasi-steady-state device) to the discharge chamber. A discharge takes place from the anode to the cathode. This may be a steady or a quasi-steady discharge. The resultant plasma is then accelerated out the nozzle by the crossed field force arising from the self field and the discharge current. For low current devices, an external field coil is required. Although the device will operate without an external field (i.e., self-induced magnetic field), it tends to be more stable at low current densities with an external coaxial solenoid. There is no fundamental space-charge limitation on the mass flow density like that arising in pure electrostatic accelerators; therefore, beam neutralization is not necessary.

B. A History of the MPD Thruster

A history of the MPD thruster must begin with early arcjet and magnetohydrodynamic (MHD) research. G. M. Giannini began work with arc-heated hydrogen engines at Plasmadyne in 1957 (Ref. 51). This early work at Plasmadyne was conducted for the Air Force Office of Scientific Research. A. Kantrowitz began experiments with arcjets and plasma acceleration at AVCO soon afterwards (Ref. 52). NASA LeRC sponsored several studies of arc-heated hydrogen engines and by 1963, AVCO, Plasmadyne, and General Electric all had developed arcjets (Refs. 53, 54, 55). MHD research began late in the 1950's. M. U. Clauser at Space Technology Laboratories began experiments with plasma acceleration at that time. These studies were later presented as a chapter in *Space Technology* by H. Seifert (Ref. 56). Electro-Optical Systems studied Hall Current Accelerators during the early 1960's (Ref. 57).

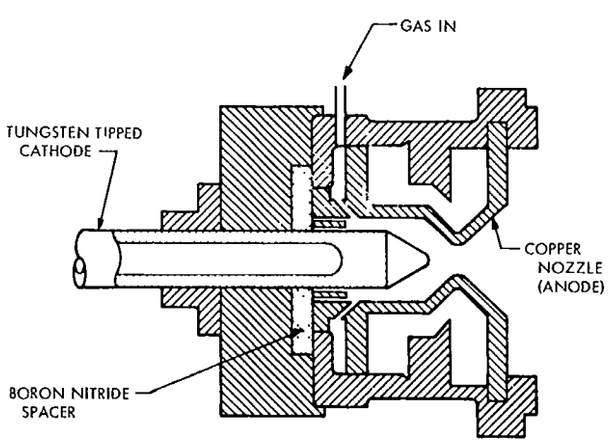

Fig. 25. Conceptual diagram of the MPD thruster

In 1963, Ducanti (Ref. 58) published data on a arcjet device called a Thermo-Ionic Accelerator. By the end of 1963, values of specific impulse up to 98,100 N-s/kg (10,000 lbf-s/ibm) with 46% efficiency were obtained with the hydrogen-fed engine (Refs. 59 and 60). The reason given for this accomplishment was the lowering of the arc chamber pressure. In addition, the supersonic nozzle that had been used to expand the electrically heated plasma in previous arcjets was removed. The device experimentally demonstrated by Giannini was the MPD arc thruster with a self-induced magnetic field. The demonstration of a MPD arc thruster provided impetus to plasma thruster research. Unfortunately, this discovery was somewhat overshadowed by the observation that thruster efficiency improved with increased test chamber pressure. The reason given is that the ambient gas in the test chamber was actually recirculated by the accelerator discharge giving false values to performance data. Arguments were then advanced that test chamber pressure was probably affecting all tests where good performance had been reported.

The testing of engines developed by AVCO and EOS at NASA LeRC has produced much useful information concerning MPD thruster operation. Avco Space Systems Division (previously AVCO/RAD) began publishing data on the self-field MPD thruster in 1964 (Ref. 61). AVCO began its experiments by trying to duplicate the results of Giannini: the use of hydrogen, ammonia, lithium, and cesium as propellants was investigated. To obtain stable operation of the self-field MPD thruster, power levels of 100 kW or greater were required. As an outgrowth of early MHD accelerator research, several laboratories began to investigate the operation of MPD thrusters with external fields. Two MPD thrusters that employ external field coils were developed by EOS and AVCO Everett Laboratories. EOS used a MPD device similar to their early Hall Current Accelerator (Ref. 62). The AVCO Everett MPD device was developed from the magnetic annular arc (MAARC) thruster (Ref. 63).

As an outgrowth of research on electron-bombardment ion thruster discharge chambers in 1962, NASA LeRC designed and tested a low-power continuous plasma accelerator (Refs. 64 and 65) applicable to auxiliary propulsion requirements. This device is sometimes referred to as the magnetic expansion thruster.

C. Characteristics of the MPD Thruster

The MPD thruster has been investigated primarily as a steady-state device; however, as mentioned earlier, it may also be pulsed. Pulsed MPD thrusters have indicated that current patterns in the exhaust plume revert to steady-state configuration after a few tens of microseconds. If a somewhat longer discharge is used, a quasi-steady operation mode is encountered. The advantages of the quasi-steady MPD will be discussed later.

The steady-state MPD thruster can operate with or without an external field. To operate in the self-induced mode, large power levels are required, for which 100 kW is typically a minimum for these devices (Ref. 66). This power level eliminates the self-field MPD arcjet from serious consideration as an auxiliary propulsion system. The MPD arcjet with an external field requires 10 to 100 kW of power for operation and thus, with one exception, is also not competitive for auxiliary propulsion. A low pressure MPD arcjet has been developed at NASA LeRC that operates at low system power.

Propellant selection is an empirical tradeoff of several considerations. The ionization potential of the propellant should be low enough to allow partial propellant ionization because only charged particles may be electromagnetically accelerated in MPD thrusters. A very low ionization potential can lead to a high degree of propellant ionization, and it is not anticipated that much of the energy invested in ionization is recovered as useful thrust. The NASA-LeRC low-power MPD arc thruster has operated with xenon, argon, carbon dioxide, and hydrogen. Xenon has been found to give the best performance (discharge power-to-thrust ratio versus specific impulse) (Ref. 67).

Most MPD arc thrusters employ a solid cathode similar in configuration to the cathode depicted in Fig. 25. More recently, some improvements in performance have resulted from the use of hollow cathodes. For example, the low-power NASA-LeRC MPD thruster employs such a device. Also, placing the hollow cathode downstream of the thruster results in increased thruster performance over the conventional upstream cathode location (Ref. 67). Unfortunately, hollow cathodes suffer from severe erosion, which tends to limit thruster life.

Early tests of MPD arc thrusters were overshadowed by the effects of test chamber pressure on thruster performance. In tests conducted at NASA LeRC, low test chamber pressures were obtained; thus the effects of entrained propellant in the test chamber have been eliminated. During testing of the low-power MPD arc thruster, test chamber pressure was altered from the nominal conditions and the results indicated no effects of test chamber pressure on thruster performance. (Ref. 67).

A variety of descriptive models for MPD arcjets have been hypothesized. The thrust from a self-induced magnetic field MPD is fairly well understood (Fig. 26).[9] The discharge current creates a self-magnetic field of strength proportional to the current. The resulting magnitude of the $j \times B_{self}$ force resulting from a self-magnetic field is therefore proportional to j^2.

[9]A thorough discussion of this subject is found in Jahn, R. G., *Physics of Electric Propulsion*, McGraw-Hill, Inc., New York, 1968.

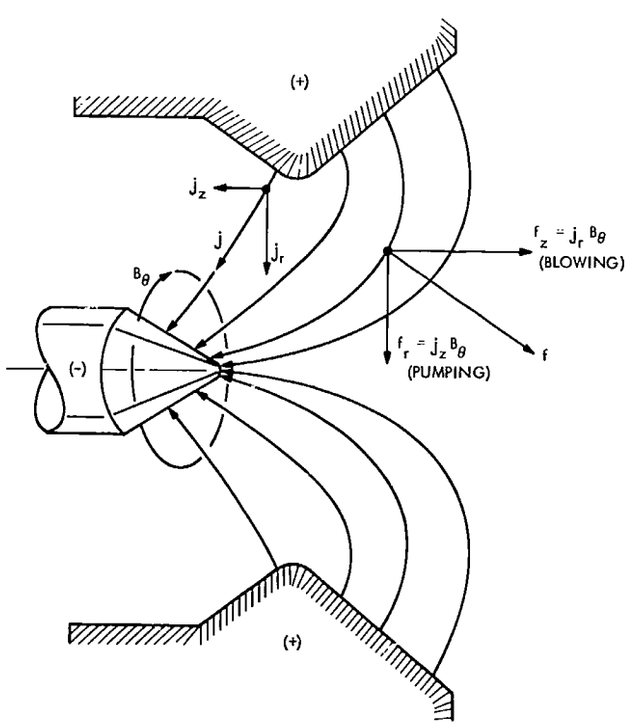

Fig. 26. Acceleration mechanism of a self-field MPD thruster

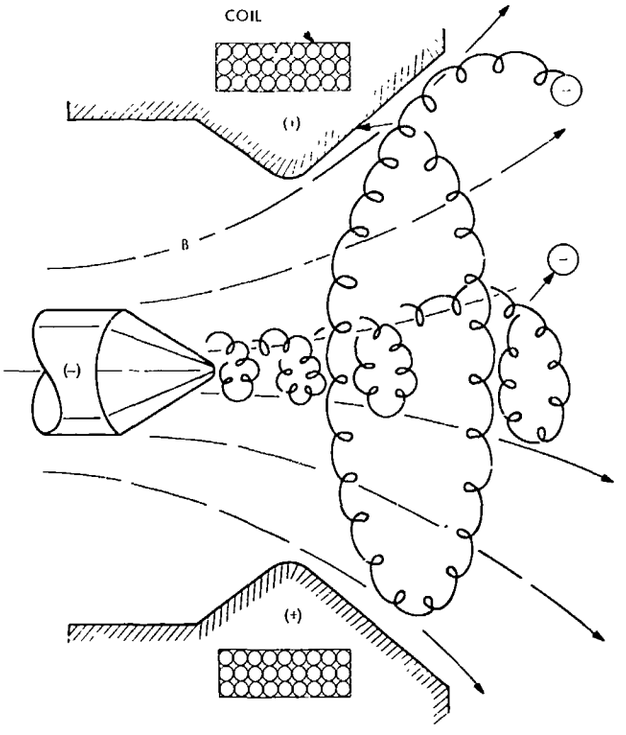

Fig. 27. Acceleration mechanism of a MPD with large external magnetic field

The effect of an external magnet upon MPD performance is not well understood, and a widely accepted model for a MPD thruster with an external magnet is not available. In general, the presence of a large external magnet causes the plasma to break into turbulent flow and becomes difficult to describe (Fig. 27).[9] Experimentally, it permits operation of the thruster at higher specific impulse without severe cathode erosion, but at slightly lower performance than the self-field MPD.

The NASA-LeRC low-power MPD thruster with external magnetic field operates according to a third descriptive model (Fig. 28).[9] A plasma with thermal electrons is formed in the discharge chamber. A magnetic funnel is generated by the external magnet. The hot electrons expand out the funnel and create an effective charge separation. The ions in the discharge chamber are then drawn into the exhaust and accelerated. This model suggests that thermal electrons can be placed into the magnetic funnel downstream of the discharge chamber, and, in fact, the most recent thrusters employ a downstream cathode. The physical model described has been verified with probe measurements. A detailed model for this thruster has been developed (Ref. 68). A direct comparison of data and theory has not been attempted yet. This is because experimenters have not been able to obtain data in the neighborhood of the sonic point because the probes were destroyed by large heat transfer in that region.

The quasi-steady state MPD thruster offers the promise of increased performance during operation because of the high current density. In addition, spaced intermittent pulses of sufficient length to obtain quasi-steady state operation allow the thruster to operate with tolerable heat transfer and low average power. The application of the quasi-steady state MPD thruster to auxiliary propulsion systems has the disadvantage of requiring a power conditioning subsystem to produce the required extended current pulses. A capacitor bank is usually employed. Typical quasi-steady state MPD thrusters require a power of 1 MW or greater for a pulse length of 1 ms. Thus, an energy of 1,000 joules is required for each pulse. The capacitor mass at 22 J/kg (10 J/lbm) becomes excessive for an auxiliary electric propulsion system. Operation of the quasi-steady state MPD thruster at power levels below 1 MW will result in decreased performance. A reduction in pulse length to below 1 ms begins to tax valve actuation time, and unless an innovative implementation is devised, a large quantity of gas will be discharged without being accelerated. Therefore, the decrease in both thruster efficiency and mass utilization that results from efforts to reduce the discharge energy below 1,000 joules still does not result in a system sufficiently attractive for auxiliary propulsion. In the future, the quasi-steady state MPD will become more attractive with decreased specific capacitor mass and the development of a highly reliable, fast-acting gas valve.

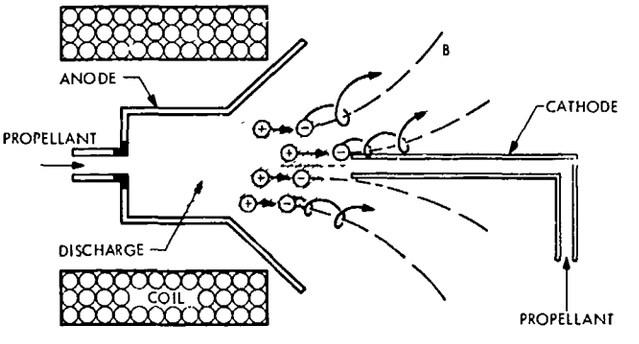

Fig. 28. Acceleration mechanism of the NASA-LeRC low-power MPD thruster (sometimes called a magnetic expansion thruster)

D. LeRC Low-Power MPD Thruster

The LeRC low-power MPD arcjet has been under development for several years (Ref. 67). The low-power MPD with upstream cathode has been operated with pure gaseous propellants (H_2, Ar, Xe) and biowaste propellants (CO_2-H_2). The most recent device incorporates a downstream cathode to improve thruster performance. Xenon has been used exclusively for tests of the downstream cathode low-power MPD. The thruster operates over a thrust range of 5.8 to 16 mN (1.3 to 3.6 mlbf) with specific impulses of 5880 to 20,590 N-s/kg (600 to 2100 lbf-s/lbm). The system is being developed for application to satellite stationkeeping and attitude control. The thruster system does not include power conditioning since it is still in the development stage. Thrust vectoring is implemented by using two pairs of off-center magnets. A slight current bias to a pair of skewed coils will create a slightly skewed magnetic field. The plasma will then be deflected off centerline, resulting in thrust vectoring of the beam. This technique has been demonstrated with an effective beam vectoring of 5 deg. The downstream cathode MPD thruster is presented in Fig. 29.

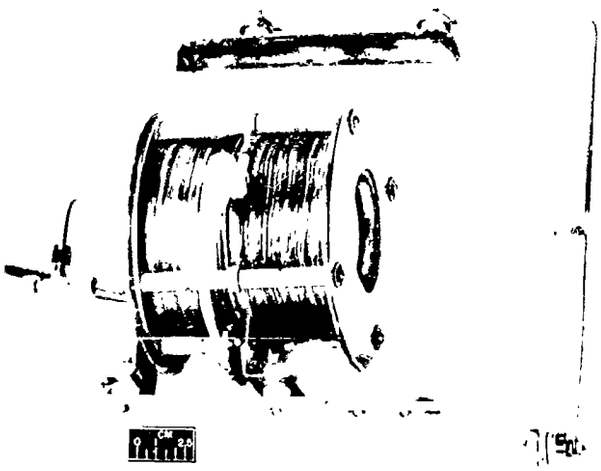

Fig. 29. NASA-LeRC low-power MPD thruster (photo courtesy of LeRC)

A schematic diagram of the thruster is presented in Fig. 30. The discharge chamber is surrounded by two electromagnets; however, in most recent tests, only the downstream edge wound electromagnet is required. A power input of 48 W was required for the downstream edge wound electromagnet. A pole piece is incorporated to intensify the magnetic field in the discharge chamber. A hollow cathode is placed in the exhaust beam downstream of the discharge chamber. The development thruster does not include a feed system, but the propellant feed system should be identical to a xenon inert gas system. Taking advantage of the compressibility of xenon at 1.0×10^7 N/m^2 (1500 psia), a pound of gas requires about 0.14 kg (0.3 lbm) of tankage. Solenoid valves have been developed for inert gas systems (e.g., Mariner) and could be used in the MPD feed system. Leakage of gaseous propellant through the solenoid is a problem, particularly during long-term storage in space. Thruster mass is approximately 2.2 kg (5 lbm) excluding the propellant feed system. Power conditioning is estimated at 3.2 kg (7 lbm) with an efficiency of 86%.

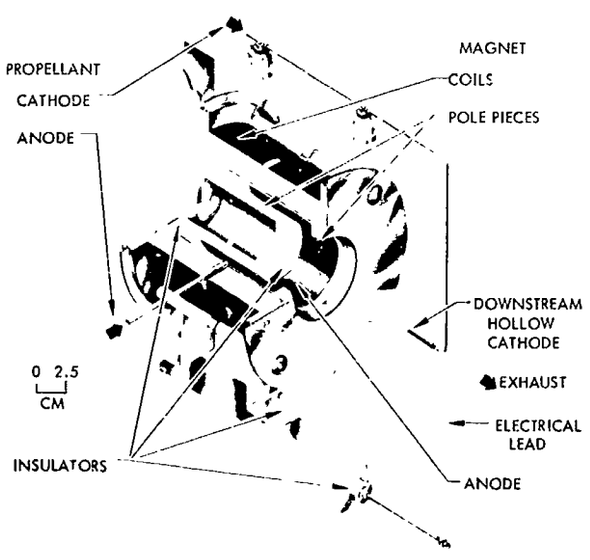

Fig. 30. Schematic of low-power MPD arc thruster with a downstream cathode

The system is capable of 4.4- to 18-mN (1- to 4-mlbf) thrust. Thrust level and efficiency increase with specific impulse. Low-power MPD performance data are presented in Table 3 (Ref. 67). The discharge chamber employs an edge wound magnet. Power to the magnet can be reduced for low-thrust, low-specific-impulse operation (12 W). Since a neutral plasma is ejected from the thruster, no neutralizer is required. A power of 1 to 3 W is required for the solenoid valve in the feed system.

At present, this system has not achieved long life. Endurance and erosion tests of an upstream hollow cathode configuration were conducted with argon as the propellant (Ref. 69). After 638 h of operation, the cathode

Table 3. Plasma thruster performance data

Thruster type	Thrust, μN (μlbf)	Thruster power, W	Specific impulse, N-s/kg (lbf-s/lbm)	Power/ thrust, W/mN (W/mlbf)	Specific thrust, μN-s/J (μlbf-s/J)	Engine efficiency, %	Power conditioning efficiency, %	Total power, W
Low-power MPD arc thruster[a]	4181 (940)	193	5296 (540)	46 (206)		5.7	86.0	224.0
	9608 (2160)	345	12,425 (1267)	36 (159)		17.3	86.0	400.0
	14,457 (3250)	625	18,456 (1882)	44 (194)		21.3	86.0	727.0
Fairchild-Hiller LES 6 thruster	16.9[b] (3.8)	1.41[c]	3040 (310)	84 (371)	13.3 (3.0)	1.8	56.0	2.52
	17.8[d] (4.0)	1.41[c]	3040 (310)	80 (353)	14.2 (3.2)	1.9	56.0	2.52
	17.3[e] (3.9)	1.41[c]	1863[e] (190)	81 (361)	13.3 (3.0)	1.2	48.0	2.91
Fairchild-Hiller[f] LES 7 thruster	398[g] (89.5)	19.6	10,081 (1028)	49 (219.0)	20.5 (4.6)	10.2	85.0	23.0
	3,85[h] (716.0)	156.8	10,081 (1028)	49 (219.0)	20.5 (4.6)	10.2	85.0	184.0
Fairchild-Hiller high energy pulsed plasma[f]	7325 (1646)[i]	257	12,200 (1245)	35 (156)	28 (6.4)	17.4	85.0	302.0
	6470 (1454)[i]	244	13,000 (1328)	37 (168)	26 (5.9)	17.2	85.0	287.0
	6600 (1483)[j]	309	18,600 (1900)	46 (208)	21 (4.8)	19.9	85.0	364.0
	3515 (790)[i]	190	32,600 (3330)	54 (241)	19 (4.2)	30.2	85.0	224.0
General Electric Solid Propellant Electric Thruster (SPET)	9[k] (2)	1.2[l]	9807 (1000)	135 (600)	9.0 (2.0)	3.6	65.0	1.8
	13[k] (3)	1.2[l]	9807 (1000)	90 (400)	13.0 (3.0)	5.5	65.0	1.8

[a]Includes 48 W for edge wound magnet power and 2 W for a solenoid valve.
[b]Reference 22 at 0.667 pps.
[c]0.1 W for telemetry.
[d]Reference 24 at 0.667 pps.
[e]Tom Williams, NASA Goddard, at 0.69 pps; one million pulses.
[f]Supplied by W. J. Guman, Fairchild-Hiller.
[g]At 1 pps.
[h]At 8 pps.
[i]At 0.531 pps.
[j]At 0.971 pps.
[k]At 1 pps.
[l]0.1 W for telemetry and 0.1 W for spark igniter.

Table 3 (contd)

Thruster type	Thrust, μN (μlbf)	Thruster power, W	Specific impulse, N-s/kg (lbf-s/lbm)	Power/ thrust, W/mN (W/mlbf)	Specific thrust, μN-s/J (μlbf-s/J)	Engine efficiency, %	Power conditioning efficiency, %	Total power, W
Pulsed vacuum arc thruster	37[k] (8.4)	4.8	4903 (500)	127.7 (567)	8.0 (1.8)	1.9	85.0	5.7
	601[m] (135.0)	76.8	4903 (500)	128.1 (569)	8.0 (1.8)	1.9	85.0	90.4
TRW pulsed inductive thruster	5769[n] (1297)	288.0	5884[p] (600)	50 (222)	20.0 (4.5)	5.9	85.0	339.0
	5769[n] (1297)	288.0	19,613 (2000)	50 (222)	20.0 (4.5)	19.6	85.0	339.0
	3674[q] (826)	200.0	5884[p] (600)	55 (242)	18.0 (4.1)	5.4	85.0	235.0
	3674[q] (826)	200.0	19,613 (2000)	55 (242)	18.0 (4.1)	17.0	85.0	235.0
	1833[r] (412)	128.0	5884[p] (600)	70 (311)	14.0 (3.2)	4.2	85.0	150.6
	1833[r] (412)	128.0	19,613 (2000)	70 (311)	14.0 (3.2)	14.0	85.0	150.6

[m]At 16 pps.
[n]12 kV on 4 μF capacitor at 1 pps.
[p]Corrected for 30% mass utilization.
[q]10 kV on 4 μF capacitor at 1 pps.
[r]8 kV on 4 μF capacitor at 1 pps.

dip had eroded 1.33 cm, leading to failure of the thruster. The cathode erosion rate has been verified by several additional life tests. At present, this form of erosion seems to be the thruster life determinant. Life tests of the downstream cathode have not yet been performed; however, cathode life is not expected to differ greatly from the previous life test data.

The initiation of thruster discharge is a problem, and at present a lightweight arc initiator for space application has not been developed. An experimental lightweight arc initiator is presently under study at LeRC.

V. Pulsed Plasma and Pulsed Inductive Thrusters

A. What Are Pulsed Plasma and Pulsed Inductive Thrusters?

The pulsed plasma thruster is a device that uses a "burst" of electrical energy to produce, accelerate, and eject a plasma wave. Pulsed plasma accelerators have electrodes in direct contact with the gas, thus requiring a zone of conducting plasma to complete the circuit, while pulsed inductive accelerators have a complex external circuit that induces a current in the gas flow. Pulsed plasma acceleration has been studied most widely, although there is some research in pulsed inductive acceleration.

Pulsed plasma devices are usually classified by their discharge chamber geometry. The parallel rail accelerator in Fig. 31a is the simplest pulsed plasma device. Two other pulsed plasma geometries are the "T tube" (Fig. 31b) and the "coaxial gun" (Fig. 31c). The pulsed inductive thruster depicted in Fig. 32 is called a "loop indicator" pulsed inductive accelerator.

The typical pulsed plasma thruster is presented in Fig 33. The propellant, a solid, liquid, or gas, is placed in the discharge gap. Solid propellant is maintained in

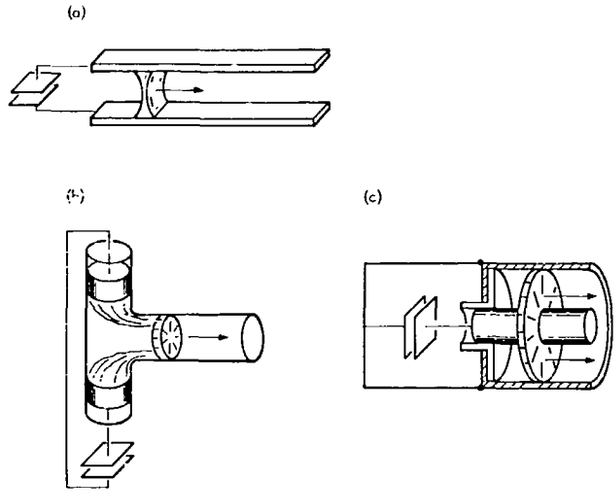

Fig. 31. Various pulsed plasma accelerators: (a) parallel-rail accelerator; (b) T tube; (c) coaxial gun (photo courtesy of R. G. Jahn in *Physics of Electric Propulsion*)

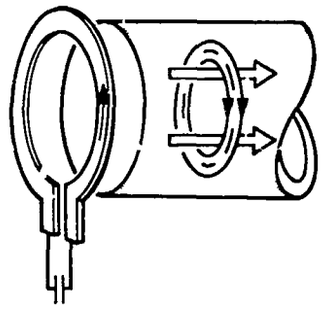

Fig. 32. Pulsed inductive accelerator loop inductor geometry (photo courtesy of R. G. Jahn in *Physics of Electric Propulsion*)

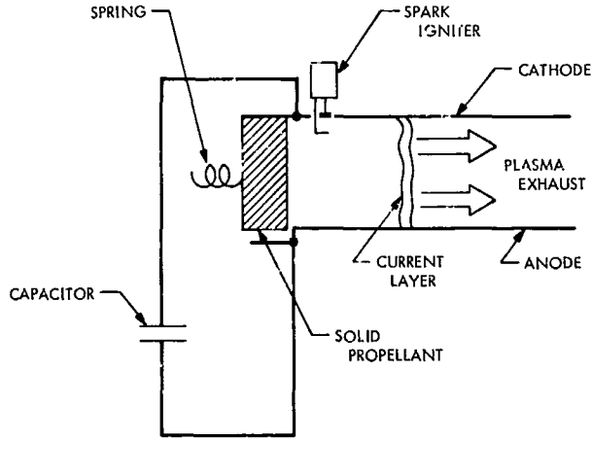

Fig. 33. Conceptual diagram of the pulsed plasma thruster

the gap region by mechanical springs, liquid is fed by capillary action, and gas is placed in chamber with a gas injection valve. A capacitor or inductor is required for energy storage. The anode-cathode configuration will vary as those presented in Fig. 15; however, the rail-type geometry is presented here. As for the MPD plasma thruster, no neutralizer is required for the pulsed plasma thruster.

The pulsed inductive thruster is similar; however, the capacitor discharge is through an inductor loop as in Fig. 34. A spark gap is required to initiate the main capacitor discharge. The propellant, usually a gas, is fed to the inductor face with a gas injection valve simultaneous to the inductor pulsing.

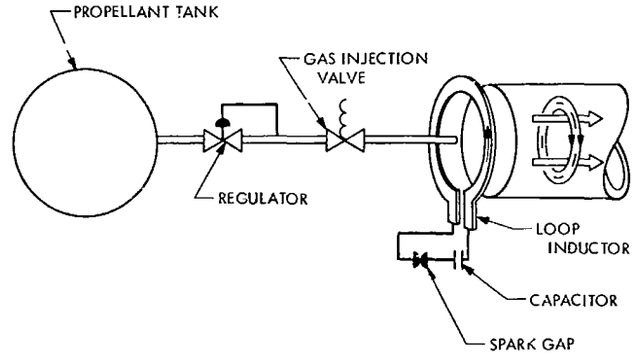

Fig. 34. Conceptual diagram of the pulsed inductive thruster

B. History of Pulsed Plasma and Pulsed Inductive Thrusters

Pulsed plasma devices have been studied for more than a decade. The earliest related studies in pulsed plasma thruster technology concerned injectors or "guns" developed in connection with the extensive program on controlled thermonuclear fusion (Ref. 70). In the late 1950's experimental studies in pulsed plasma thrusters were initiated by several laboratories (Refs. 71, 72, and 73). By 1965 General Electric Company (Ref. 74), General Dynamics Corporation (Ref. 75), Rocket Research Corporation (Ref. 71), and Republic Aviation Corporation (Ref. 76) had developed gaseous propellant pulsed plasma thrusters.

Solid propellant pulsed plasma acceleration research began in 1956 (Ref. 77). For a history of early solid propellant pulsed plasma thrusters see Ref. 78. By 1966

solid propellant pulsed plasma thrusters were developed by Republic Aviation (Ref. 78), General Electric (Ref. 79) and Cornell Laboratories (Ref. 80).

Pulsed inductive plasma accelerators have been studied for some time, with early non-thruster oriented research. By 1965 C. L. Dailey had developed a pulsed inductive plasma accelerator applicable for auxiliary propulsion (Ref. 81).

C. Characteristics of Pulsed Plasma and Pulsed Inductive Thrusters

Pulsed plasma thrusters rely on three physical events to obtain thrust:

(1) Discharge initiation.

(2) Plasma acceleration.

(3) Plasma ejection.

The initiation event will occur at portions of the channel (Fig. 33) nearest the external circuit. The discharge begins as an abnormal glow and progresses toward an arc. A small expenditure of energy compared to the acceleration process and minimum erosion of electrode surfaces are requirements of the breakdown event. The initiation is usually accomplished in two stages with a small spark igniter supplying ionized gas to the channel prior to the main discharge.

Acceleration of the gas relies on $j \times B$ forces arising from the discharge current and its self-magnetic field. The "current layer" formed during the initiation phase of thrusting acts as a piston to accelerate the plasma.

As the plasma reaches the physical end of the channel it begins the ejection phase of thrusting. The process of expelling plasma from the channel is difficult to analyze. It has been shown that current densities and associated magnetic fields can extend far into the exhaust plume, and can aid in further acceleration of the gas. In addition to magnetic acceleration during the ejection phase, an expansion nozzle will aid in the recovery of gas dynamic pressure forces and serve to convert thermal energy to kinetic energy. If the majority of the thrust is derived from magnetic rather than gas dynamic pressure forces, which is generally the case, then the addition of an expansion nozzle will not improve thruster performance.

The pulsed inductive plasma thruster relies on four physical events to obtain thrust:

(1) External initiator.

(2) "Secondary current" creation.

(3) Plasma acceleration.

(4) Plasma ejection.

A switch (i.e., spark gap) is employed to complete the external primary circuit. Current from the storage capacitor flows through a large inductor, creating a rapidly growing magnetic field.

Because of Maxwell's induction equation, an electric field must arise from the external magnetic field. The net effect of the rapidly growing magnetic field is the inducement of a "secondary current" in the gas that has been placed near the inductor.

The acceleration of the resulting plasma gas arises from the interaction of the secondary current and the external magnetic field. As before, the force of acceleration is proportional to the secondary current density times the external magnetic field ($j \times B$).

Ejection of the plasma from a pulsed inductive thruster is similar to that of a pulsed plasma thruster, and the addition of a nozzle for recovery of gas dynamic pressures is not necessary because they are for the most part small compared to magnetic acceleration forces.

Pulsed plasma and pulsed inductive thrusters have been operated with a variety of propellants. Gaseous propellants have received a great deal of attention. The gas present in the thruster during pulsing can be utilized directly for thrust, while the gas that escapes prior to pulsing, and the gas supplied after the electrical pulse, cannot be fully utilized. The percentage of gas effectively accelerated, mass utilization efficiency, is low for gaseous pulsed plasma thrusters because the duration of the electrical pulse is short (1 to 5 μs) in comparison with valve actuation time. The design of a solenoid valve with a rapid on-off time, good vacuum seal, and one that is reliable for millions of cycles is a difficult problem. One good feature of gaseous propellant is that no energy is required to vaporize the propellant, thus improving thruster efficiency.

Liquid propellants have been investigated as a means of removing the solenoid valve from the total thruster system. Liquid (e.g. mercury) can be retained in a cavity

by surface tension, and fed by capillary action to an evaporation surface. Problems with liquid propellants include continual evaporation of propellant from the liquid-vacuum surface that can result in considerable propellant loss during long missions, and the difficult control of capillary feeding of propellant. Also some energy must be invested in propellant vaporization, and this energy is not returned as useful thrust.

Solid propellants tend to go one step further in the removal of solenoid valves from pulsed plasma thrusters. The continual evaporation of propellant from the solid propellant-vacuum surface is minimal and can be ignored. However, as before, some energy must be invested in propellant sublimation, thus adding to thruster inefficiency.

The mass acceleration mechanism of pulsed plasma thrusters is difficult to measure because the thruster's operation is dynamic. Early experimenters relied on time-of-flight measurements to determine thruster efficiency and specific impulse. Recently, it has been shown that time-of-flight data is not valid for the measurement of pulsed plasma system performance, because a rather low mass utilization efficiency is observed for pulsed plasma thrusters. The majority of the propellant is expelled at low velocity without being ionized. Only ionized particles at high velocity are measured in time-of-flight data; the neutral particles at low velocity escape uncounted.

The measured performance of pulsed plasma thrusters seems to improve with increasing specific impulse. Early studies of coaxial gaseous pulsed plasma thrusters reported high thruster performance; however, this high performance was at 49,000-N-s/kg (5000-lbf-s/lbm) specific impulse. Power requirements for a high specific impulse pulsed plasma thruster increase above the propellant savings for high specific impulse auxiliary propulsion, so presently pulsed plasma thrusters are usually limited to 29,400-N-s/kg (3000-lbf-s/lbm) specific impulse.

Gas valve studies are continuing in an effort to improve the mass utilization of gaseous propellant thrusters; however, no new unique valve designs have been developed. As an effort to increase the mass utilization of solid propellant pulsed plasma thrusters, the introduction of propellant along the path of the pulsed current sheet is being studied. Also "chopping" of the discharge after the initial high current density pulse will reduce the tailoff emission of neutral propellant.

Experiments with quasi-steady state MPD thrusters have suggested that a quasi-steady operation of pulsed plasma thrusters may increase thruster performance. Quasi-steady operation can be achieved with capacitor banks; however, the length of quasi-steady operation that will offer maximum system performance is not known yet. Also the mass of additional capacitors may become excessive for auxiliary propulsion systems.

Three types of capacitors that have been investigated for pulsed plasma thrusters are:

(1) Thin-film plastic with or without dielectric fluid impregnation.

(2) Paper impregnated with fluid.

(3) Electrolytic.

The ohmic losses of the thin-film plastic and paper capacitors are much lower than losses in electrolytic capacitors. With rapid discharge of capacitor energy, the ohmic losses in electrolytic capacitors generate considerable internal heat. Tests of electrolytic capacitors at pulsed plasma discharge times (1 to 10 μs) have ended in capacitor destruction because of excessive heat generation. It is for this reason that electrolytic capacitors are not competitive for rapid discharge pulse plasma thrusters.

Present state-of-the-art capacitors have an approximate specific mass of 13 to 22 J/kg. This specific mass is arrived at by derating a high voltage capacitor. Capacitor derating is sufficient to allow 10^7 pulses at high reliability.

Radio frequency interference (RFI) has been observed on pulsed plasma thrusters. Measurements of RFI noise have been taken on UHF and X-band frequency; similar measurements at the time of this writing are being taken on S-band frequency. Measurements on the LES-6 pulsed plasma thruster (1.85 J discharge) indicate some RFI at UHF frequencies (Ref. 82). Recent measurements of a higher power (20 J discharge) pulsed plasma thruster have indicated that considerable RFI noise is present during the 1 to 3 μs discharge (Ref. 83). The increase in RFI noise with thruster discharge energy indicates that considerable noise can be generated in high power pulsed plasma thrusters. Noise suppression can be achieved with a wave guide, although the geometry of the thruster (diameter of exit) does not allow efficient suppression of radio frequency noise. The effect of a short duration "burst" of RFI noise of spacecraft operation is a function of the type of data transferred. RFI noise is not as critical

to television and radio transmission as it is to sequenced commands. The effects of RFI noise on spacecraft operation at present are not well understood.

D. Space Experience of Pulsed Plasma Thrusters

A solid-propellant pulsed plasma propulsion system having four thrusters was launched aboard the MIT Lincoln Laboratory LES-6 Satellite in September 1968 (Ref. 84). After more than 2 years in space, the pulsed plasma thrusters continue to function well. In a simulated life test at vacuum facilities, intermittency or failure to discharge capacitor energy was observed. The intermittency would not correct itself and the unit stopped firing completely. After more than 3 million pulses on each of the four flight thrusters, intermittency has been observed in three of the four thruster units. Complete failure (100% intermittency) has occurred to only one thruster unit. More recent designs have corrected this intermittency problem. The propulsion system has functionally kept the LES-6 Satellite within the ±2-deg longitude design band (Ref. 85).

E. Fairchild-Hiller LES-6 Pulsed Plasma Thruster

Republic Aviation Division of Fairchild-Hiller Corporation has developed a solid-propellant pulsed plasma thruster for the MIT Lincoln Laboratories, LES-6 (Refs. 84 and 86). This thruster is capable of providing a 27-μN (6-μlbf-s) impulse bit per discharge of the 2-μF capacitor. The flight system is charged to 1360 V, which is equivalent to a 1.85-joule discharge. A solid block of Teflon is used as propellant. The thruster system is complete with feed system, power conditioning, and telemetry circuits. This system does not have thrust vectoring capability. The LES-6 thruster is presented in Fig. 35.

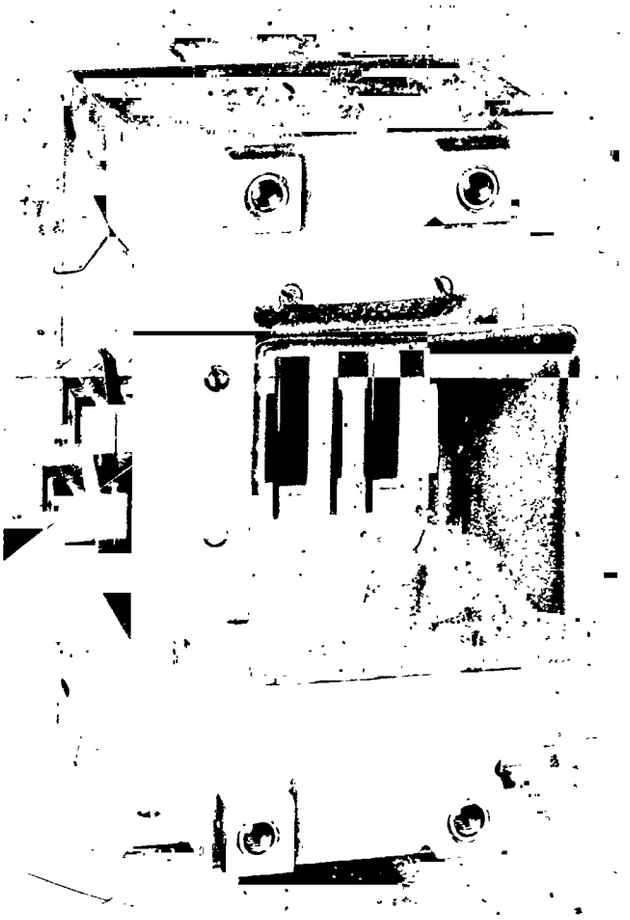

Fig. 35. Fairchild-Hiller LES-6 pulsed plasma thruster (photo courtesy of Fairchild-Hiller)

A schematic diagram of the solid-propellant LES-6 pulsed plasma thruster is presented in Fig. 36. A small capacitor discharge (⅛ joule) across the spark igniter provides sufficient plasma to initiate a discharge between the anode and cathode. The main discharge evaporates, ionizes, and accelerates Teflon propellant. A spring is employed to feed the Teflon to the thruster. A retaining shoulder maintains the propellant between the anode and cathode. Open failure of valved liquid or gaseous systems can lead to forces or moments applied to the spacecraft. Solid Teflon propellant remains passive when not used, or in the event of a failure. The LES-6 thruster configuration employs one 2-μF capacitor and two separate anode, cathode, spark igniter and propellant subsystems. The two complete subsystems provide redundancy with little addition to total mass. Each thruster

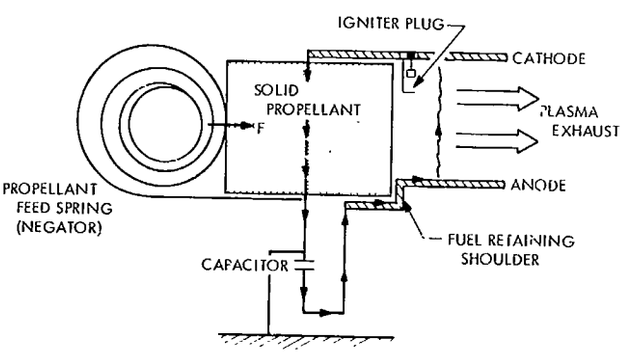

Fig. 36. LES-6 thruster schematic

system, including case and Teflon propellant, has a mass of 1.4 kg (3.0 lbm). Each thruster includes 0.1 kg (0.3 lbm) of Teflon, which provides 280-N-s (64-lbf-s) total impulse. A power conditioner was developed which

provides 1.32 W of power to the main and igniter capacitors of any of four thruster units. The conditioner has a mass of 0.9 kg (1.9 lbm) and has an efficiency of 56%.

The thruster can operate at several discharge energies and different pulse rates. The nominal discharge energy of 1.85 joules provides 25- to 27-μN-s (5.7- to 6.0-μlbf-s) impulse bit per discharge (Refs. 84 and 86). Measurements in space suggest that 24-μN-s (5.35-μlbf-s) impulse bit per discharge is achieved for this thruster.[10] Typical performance data are presented in Table 3.

Radio frequency interference noise has been observed on the LES-6 thrusters. Measurements of this noise are discussed in Ref. 82. These measurements are presented in Fig. 37, where noise is expressed as power per Hz as a function of time from capacitor discharge. This noise has not affected normal operation of the LES-6 satellite.

Prototypes of the LES-6 thruster designed in 1968 were tested extensively in the laboratory (Ref. 84). Ground testing was performed at 1 to 4 pps. On several tests the thruster achieved more than 8 million discharges without failure of the capacitor or discharge initiator. Intermittency of discharge to occur is common with the flight thruster after 1 to 2 million discharges. An intermittent thruster does not draw power, and thus the capacitor can be discharged later. However, when the intermittency becomes more frequent the thruster may never recover. During tests of the LES-6 pulsed plasma thruster at Lincoln Laboratories, one thruster became intermittent after 1 million pulses and did not recover.[11]

F. Fairchild-Hiller LES-7 Pulsed Plasma Thruster

This thruster was developed for use on the LES-7; however, the planned spacecraft has been cancelled (Ref. 87). This thruster is capable of providing a 270- to 400-μN (60- to 90-μlbf-s) impulse bit per discharge of the capacitor. This is a scaled-up version of the LES-6 thruster. The performance of the device increases with discharge energy. The thruster is complete with feed system. The two thrusters per capacitor are skewed with respect to each other, providing thrust vector control. The LES-7 thruster system is depicted in Fig. 38.

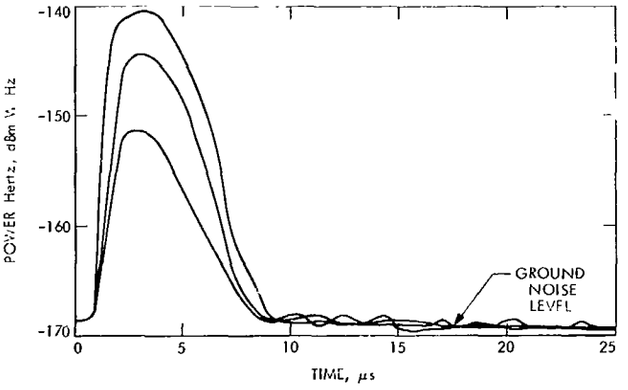

Fig. 37. Radio frequency interference from a LES-6 thruster at UHF frequency

Fig. 38. LES-7 pulsed plasma thruster (photo courtesy of Fairchild-Hiller)

Features of the thruster are similar to those described in the LES-6 system. Two igniter plugs are provided in each of the two nozzles and the parallel accelerators are skewed 30 deg to each other as depicted in Fig. 38. Total thruster mass is 4.8 kg (10.5 lbm) with 0.7 kg (1.6 lbm) of Teflon propellant included in each system. A 1.3-kg (2.9-lbm) power conditioner with 85% electrical efficiency is estimated[12] to be capable of providing 20 to 40 W of conditioned power to the thruster.

Typical performance data are presented in Table 3. The specific impulse of this thruster is near 9800 N-s/kg (1000 lbf-s/lbm), three times greater than that of the

[10]D. C. MacLellan, MIT Lincoln Laboratory, personal communication.

[11]D. C. MacLellan, MIT Lincoln Laboratory, personal communication.

[12]Mannie Landsman, MIT Lincoln Laboratory, personal communication.

LES-6 thruster. This improvement was due to increased discharge energy, increased Teflon surface area, and small changes in nozzle geometry. Included also in the performance table are four experimental data points from a high-power, high-impulse-bit, pulsed plasma thruster for north-south stationkeeping. The four high-discharge energy data points are experimental and are averaged over at least 4 h of continuous operation. The two data points with high specific thrust employ side feed of Teflon.

Radio frequency interference (RFI) noise seems to increase with discharge energy; RFI measurements from an experimental thruster similar to the LES-7 pulsed plasma thruster indicate a much higher level of noise than observed in the LES-6 thrusters (Ref. 88). Measurements of X-band frequency RFI noise are presented in Fig. 39.

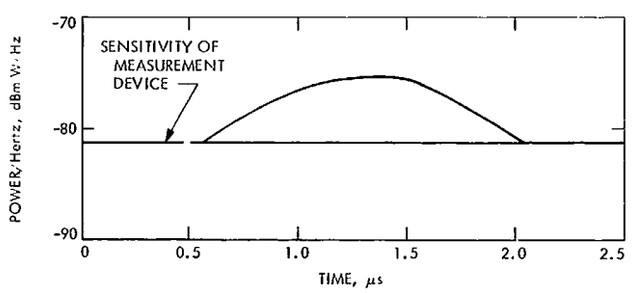

Fig. 39. Radio frequency interference from an early LES-7-type thruster

Life tests of thrusters resembling the LES-7 thruster configuration have been performed (Ref. 88). These tests suggest that 5 to 10 million pulses can be achieved without thruster failure. The problem of feeding large quantities of Teflon to the high-power, high-impulse-bit thruster has been analyzed and shown to be feasible (Ref. 87). Coiling of Teflon propellant and feeding by springs has been suggested. However, the problem of possible Teflon binding in the coiled position after long storage times is presently unresolved. Some life testing of this feed system is required before it can be used in space.

G. General Electric Solid Propellant Electric Thruster (SPET)

General Electric Company has developed several solid propellant pulsed plasma thrusters. The most recent design is called the "inside-out" SPET (Ref. 89). This coaxial pulsed plasma thruster uses a "wax-like" perfluorocarbon propellant, which behaves like a high viscosity liquid. The propellant is supplied by capillary feed to the outer electrode (Fig. 40). This thruster is capable of providing a 13- to 330-μN-s (3- to 75-μlbf-s) impulse bit per discharge of the 0.25- to 7.6-μF capacitor. The system (0.5 μF) is charged to 2000 V, which is equivalent to a 1.0-J discharge providing an impulse bit of 13 μN-s (3 μlbf-s). The thruster system is complete with propellant storage tank, capacitors, and power conditioning. The system does not have thrust vectoring capability. A SPET thruster is depicted in Fig. 41.

A small discharge (1/10 J) across the spark igniter (Fig. 40) provides sufficient conductive material to initiate a discharge between the anode and cathode.

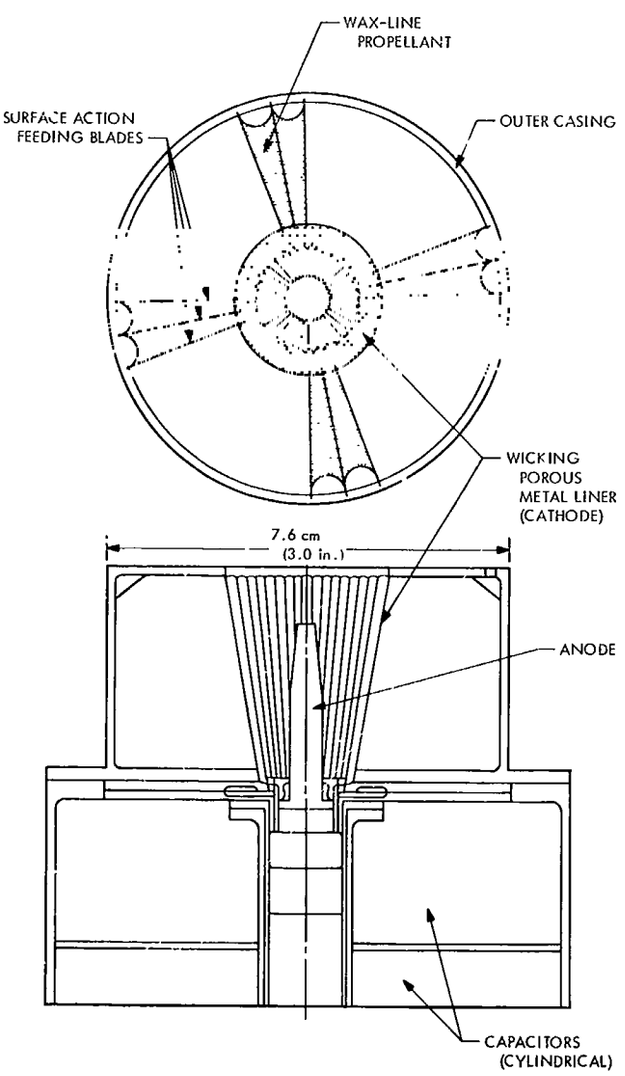

Fig. 40. Solid propellant electric thruster (SPET) schematic

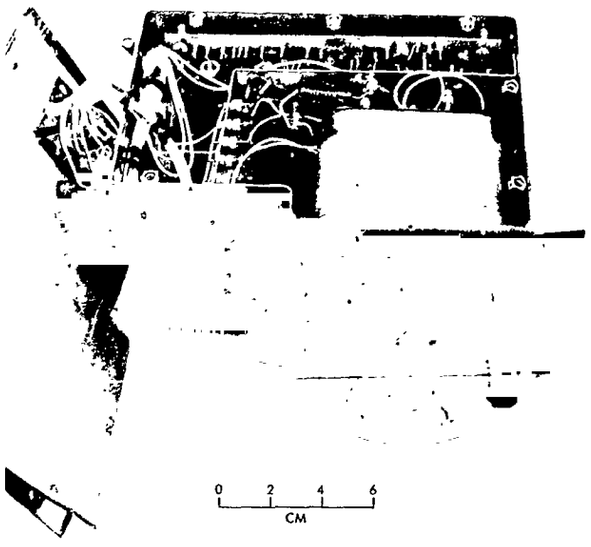

Fig. 41. SPET pulsed plasma thruster (photo cour. of General Electric)

The main discharge evaporates, ionizes and accelerates the propellant as it passes over the capillary wick surface. The evaporation rate and feed rate of the propellant is an important factor in efficient thruster operation. Thermal effects on propellant feed and evaporation rate are not well understood. A complete thruster package including structure has a mass of 0.6 kg (1.4 lbm). This includes 0.05 kg (0.1 lbm) of usable propellant, which provides 445-N-s (100-lbf-s) total impulse. A power conditioner is included to provide 1 W of conditioned power. The power conditioner has a mass of 0.5 kg (1.2 lbm) and an efficiency of 65%.

The thruster can operate at several discharge energies and different pulse rates. The nominal discharge energy of 1.0 J provides a 9- to 13-μN-s (2- to 3-μlbf-s) impulse per discharge.[13] A specific impulse of around 9800 N-s/kg (1000 lbf-s/lbm) is achieved for this thruster. Typical performance data are presented in Table 3. The specific impulse measurement was obtained over a 24 h period.

No RFI noise measurements have been made on the "inside-out" SPET. Measurements of RFI noise were made on an earlier version of the SPET thruster. Interference noise was detected up to a frequency of 100 MHz from the SPET A system (Ref. 90). No RFI noise was recorded at L, S, or X band frequencies.

[13]A. V. LaRocca, General Electric Company, personal communication.

No life testing has been performed on the "inside-out" thruster; however, testing of this thruster at NASA Goddard, at the time of this writing, is underway. Life tests of an earlier version SPET thruster have provided data on three thrusters that surpassed 5 million pulses (Ref. 89). The spark gap igniter has been tested separately for more than 10^8 discharges without failure.

H. Pulsed Vacuum-Arc Thruster (PVAT)

This thruster, originally developed at Cornell Aeronautical Laboratory, uses a zinc wire for propellant (Ref. 91). The wire serves as a cathode as well as the propellant. The thruster provides a 37-μN-s (8.4-μlbf-s) impulse bit per discharge of the 240-μF capacitor. The system is charged to 200 V, which is equivalent to a 4.8-J discharge. The system is complete with coiled zinc wire propellant, capacitors and magnetic coils that can provide $\pm 10°$ thrust vector control. The pulsed vacuum-arc thruster is depicted in Fig. 42.

A small discharge (fraction of a joule) between an igniter electrode and the end of a zinc wire (cathode) provides sufficient conductive material to initiate the discharge of the main energy storage capacitor between the anode and cathode (Fig. 43). The device has a magnetic field coil in a series connection with the electrodes in the main discharge. The zinc wire is fed to the tip of

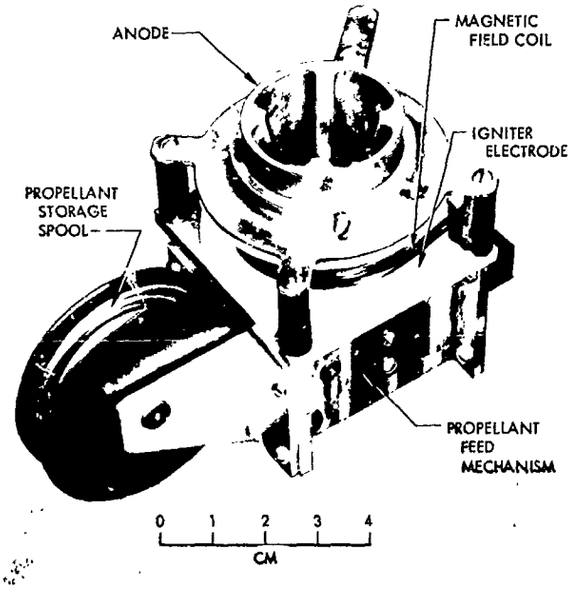

Fig. 42. Pulsed vacuum arc thruster (PVAC) (photo courtesy of David Lockwood)

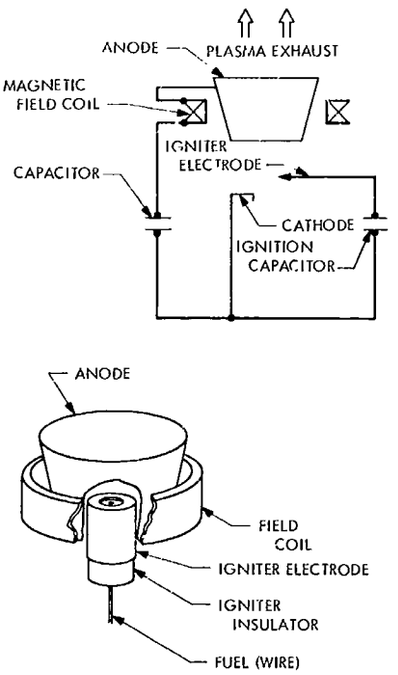

Fig. 43. Pulsed vacuum-arc thruster schematic

an insulator as depicted in Fig. 44. Erosion of the insulator is severe, so a tapered zinc wire is employed to match the insulator erosion rate. Some problems with this feed system have been encountered after a few million pulses (igniter-to-cathode shorts, and excessive igniter insulator erosion). The complete thruster system has a mass of 4.5 kg (10 lbm). This includes 0.2 kg (0.4 lbm) of zinc propellant. A power conditioning mass of 2.3 kg (5 lbm) and an efficiency of 85% is estimated for this thruster.

The thruster can operate at several discharge energies and different pulse rates. Recent thrust stand data have indicated that earlier measurements based on time-of-flight data may yield erroneous performance data (Ref. 92). The system can be operated with a 240-μF capacitor

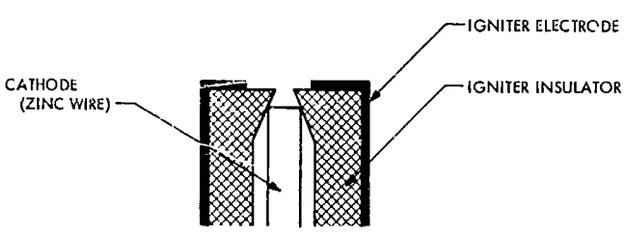

Fig. 44. Detail of cathode portion of the PVAT

charged to 200 V (4.8 J per discharge). Thrust stand measurements (Ref. 92) indicate 37-μN-s (8.4-μlbf-s) impulse bit per discharge when operated at 16 pps. A specific impulse of 4900 N-s/kg (500 lbf-s/lbm) is recorded. Typical system performance data are presented in Table 3.

No RFI noise measurements have been performed on this thruster. Several thrusters were life tested (Ref. 93). Failure of the igniter-feed system was recorded after 1 to 10 million discharges. The problem in most cases was severe erosion of the igniter insulator, leading to release of the zinc wire. In all cases the capacitor system worked well, and experienced no failures.

I. TRW Pulsed Inductive Thruster

TRW Systems Group has developed a pulsed inductive thruster (Ref. 94). This thruster uses a variety of gaseous propellants; however, xenon will be discussed herein. A fast-opening gas-injection valve is employed to feed propellant to the thruster. The propellant does not form a zone of conducting plasma to complete the primary circuit as in pulsed plasma thrusters. A 20-cm (8-in.) flat spiral coil is used to induce a current sheet in the propellant. A 4-μF capacitor charged to a voltage of 6 to 12 kV is discharged across the spiral coil. This thruster provides a nominal 4.45-mN-s (1-mlbf-s) impulse bit per discharge. The thruster system is complete with gas-injection valve, field coil, ignition circuit, and capacitor. The thruster assembly, mounted on a thrust balance, is presented in Fig. 45.

Gas is fed from a storage tank to a small plenum upstream of the gas-injection valve (see Fig. 46). A small capacitor is discharged across the fast-acting valve along with the initiation of a delay generator. A variable delayed trigger pulse is sent to the spark gap several hundred μs after valve initiation, when gas distribution over the coil is at a maximum. The capacitor then discharges through the spark gap and thruster coil. The mass utilization, or percentage of injected gas distributed over the valve during the acceleration phase, is only 30%. This is due to the long valve actuation time ($\sim$800 μs) compared to the short time for the thruster acceleration process (10 μs). A delay of about 600 μs before thruster acceleration begins is typical for this system. A complete thruster package including 4-μF capacitor, thruster valve, 20-cm coil, trigger, and solenoid capacitor has a mass of 11.4 kg (25.0 lbm). A mass of 0.1 kg (0.3 lbm) can be estimated for a regulator, and 0.1 kg (0.3 lbm) of tankage can be assumed for each

Fig. 45. TRW pulsed inductive thruster (photo courtesy of TRW Systems Group)

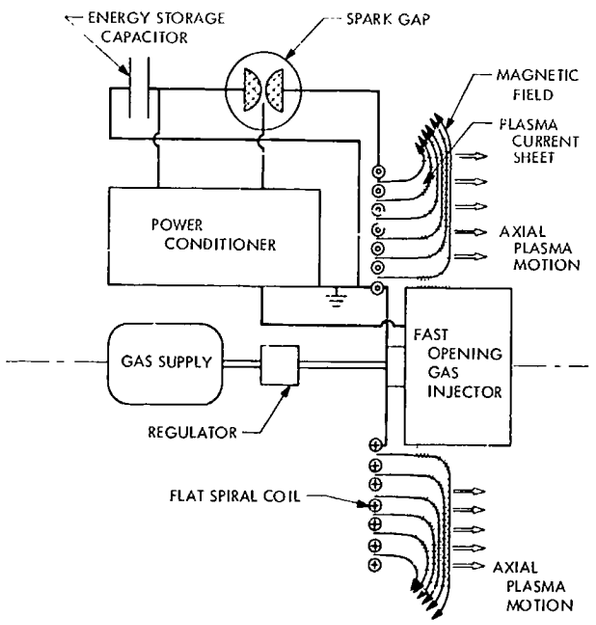

Fig. 46. Pulsed inductive thruster schematic

0.5 kg (1 lbm) of Xe propellant at 10×10^6 N/m² (1500 psia). Power conditioning mass is estimated at 3.1 kg (6.8 lbm) with an efficiency of 85%.

The thruster can operate at several discharge energies and different pulse rates. The nominal discharge energy of 200 joules (10 kV) provides 3.7-mN-s (826-μlbf-s) impulse bit per discharge (Ref. 94). A specific impulse of 19,600 N-s/kg (2000 lbf-s/lbm) has been measured; however, it should be corrected to include the 30% mass utilization efficiency. Typical performance data are presented in Table 3.

To date of this writing, no RFI noise or life test data are available. Present efforts are underway to improve the performance and mass utilization of this thruster.

VI. Conclusions Based On Demonsrrated Life, Mass, Performance, and Power

The spacecraft systems engineer when faced with the selection or integration of an auxiliary-electric propulsion system for application to a mission will first ask: What is the system mass? What is the thrust level? How much total impulse has it demonstrated? How much power does it require? These questions can best be answered by summarizing the contents of the preceding auxiliary-electric thruster survey. The thruster systems surveyed can be divided into two groups: microthrusters and north-south stationkeeping thrusters.

Microthrusters are low-thrust (e.g., 0 to 223-μN) devices capable of providing thrust for spacecraft attitude control, orientation, east-west stationkeeping, and momentum wheel unloading. The total impulse requirements of microthruster systems may be as much as 4400 N-s (1000 lbf-s).

The second group of auxiliary-electric thrusters is the one considered for north-south stationkeeping and other spacecraft propulsion requirements such as orbit modifications. Satellite size will serve to define a minimum thrust for north-south stationkeeping thrusters. For each 454 kg (1000 lbm) of spacecraft, a minimum of 670-μN (150-μlbf) thrust is required if the north-south stationkeeping thruster is *on* 100% of the time. Thus north-south stationkeeping thrusters fall into a thrust range of 450 μN to 4.5 mN (100 μlbf to 1 mlbf), where the low-thrust range is applicable only to satellites below 454 kg (1000 lbm). A total impulse of 21,000 N-s (4730 lbf-s) per year is required for each 454 kg (1000 lbm) of spacecraft mass. If orbit corrections are required, the time required for orbit correction and the amount of spacecraft movement will define thruster requirements (Fig. 47) (Ref. 95).

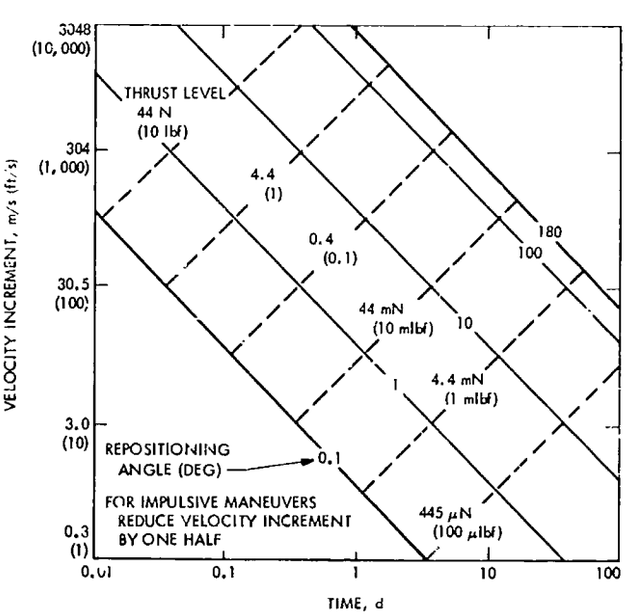

Fig. 47. Propulsion requirements for synchronous satellite orbit correction by low-thrust auxiliary electric thrusters (Ref. 95)

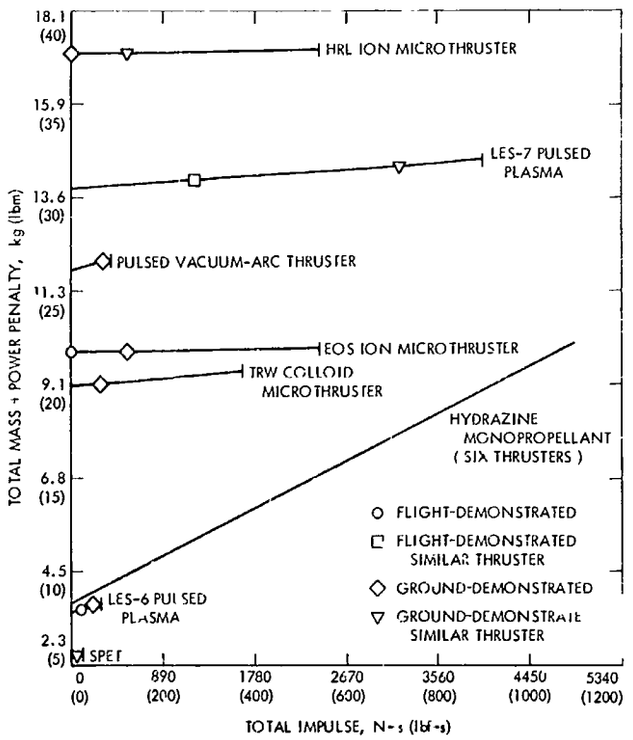

Fig. 48. Mass of microthruster systems (two thrusters per system, each capable of the plotted total impulse)

Thruster systems are compared on plots of total thruster system mass as a function of the total impulse required (Figs. 48 and 49). The total mass shown includes a power penalty of 0.1 kg/W (solar cells at ~3 W/lbm). Shown for comparison on these plots is a 450-mN (100-mlbf) monopropellant hydrazine system sized for the same functions. All electric thruster systems include two complete thrusters, power conditioning, and propellant. The demonstrated total impulse has been separated into four categories:

(1) Flight-demonstrated thruster life.

(2) Flight-demonstrated life of a similar-type thruster.

(3) Ground-simulated life tests in high vacuum.

(4) Ground-simulated life tests of a similar-type thruster.

The total impulse plotted is per thruster. Since there are two thrusters per system, the spacecraft will therefore receive twice the plotted total impulse if both thrusters use all their propellant. For a comparison of thruster total impulse capability, each thruster mass line has been terminated with an end point that corresponds to 10,000 h for steady-state thrusters and 10,000,000 pulses for pulsed thrusters. The life estimate of the high-energy plasma thrusters was set at 20,000,000 pulses.

Auxiliary-electric microthrusters surveyed include the Hughes Research Laboratory and Electro Optical Systems cesium contact-ion thrusters, the TRW Systems Group colloid microthruster, the Fairchild-Hiller LES-6 and LES-7 pulsed plasma thrusters, the General Electric SPET, and the Pulsed Vacuum-Arc thruster. Several conclusions can be drawn on microthruster systems (Fig. 48):

(1) The ion (HRL and EOS) and colloid microthrusters in general have greater fixed mass (including penalty for power) than the pulsed plasma microthrusters.

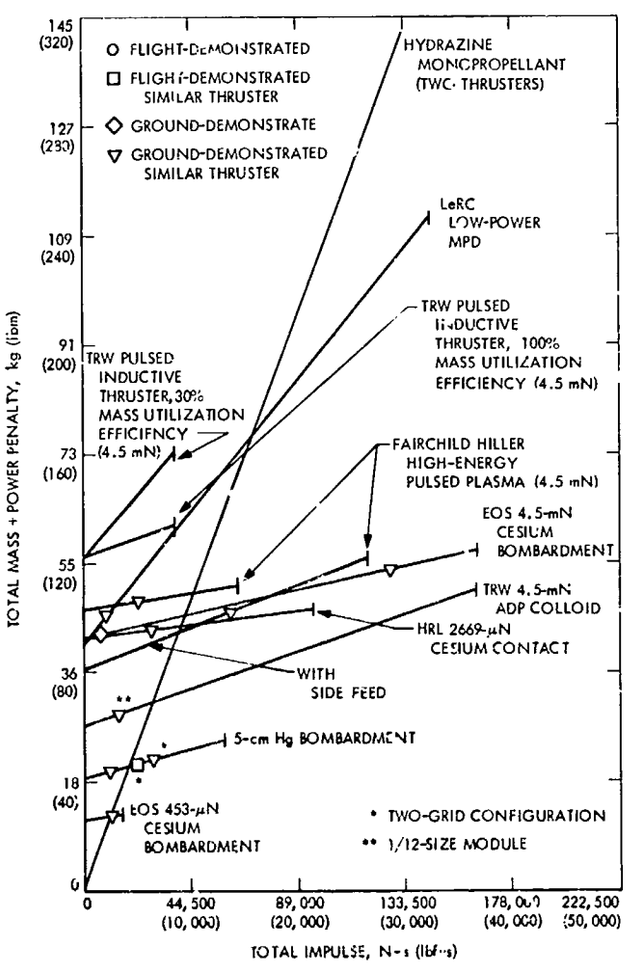

Fig. 49. Mass of complete north-south stationkeeping thruster systems (two thrusters per system, each capable of the plotted total impulse)

(2) Demonstrated life of the pulsed plasma system exceeds the other auxiliary-electric microthrusters.

(3) For three-axis-stabilized spacecraft, either two electric microthrusters with beam deflection (e.g., ion microthrusters), or six monopropellant hydrazine thrusters could provide east-west stationkeeping.

(4) The mass of the hydrazine catalyst system with six thrusters is less than the mass of any of the electric microthrusters, with the exception of the low-total-impulse (450-N-s) pulsed plasma thrusters.

(5) Pulsed plasma thrusters should be considered for spinning satellites and other spacecraft that require extensive pulsing.

Auxiliary-electric thrusters surveyed, which are suitable for north-south stationkeeping, are the HRL 2.7-mN (600-μlbf) linear strip ion thruster, the EOS 450-μN (100-μlbf) and 4.5-mN (1-mlbf) cesium bombardment thrusters, the HRL and LeRC 5-cm Hg bombardment thruster, the TRW 4.5-mN (1-mlbf) ADP colloid thruster, the LeRC low-power MPD, Fairchild Hiller's experimental pulsed plasma, and TRW's pulsed inductive thruster. The following conclusions are drawn for auxiliary-electric north-south stationkeeping thrusters (Fig. 49):

(1) The EOS 450-μN (100-μlbf) cesium bombardment thruster for low-total-impulse requirements (small satellites) offers a small mass advantage over monopropellant hydrazine, when the thruster is sized for its assumed maximum capability. Below that size, it is heavier than an equivalent hydrazine system.

(2) The 5-cm mercury bombardment thruster offers some improvements over a hydrazine system above 22,250-N-s (5,000-lbf-s) total impulse. Present demonstrated life of glass grids is less than 22,250-N-s (5000-lbf-s) total impulse; however, the SERT II life tests indicate possible long life with a two-grid arrangement.

(3) The 4.5-mN (1-mlbf) colloid thruster offers the greatest mass savings of any of the auxiliary-propulsion systems plotted for missions with total impulse requirements of more than 66,750 N-s (15,000 lbf-s). The mass of the 4.5-mN (1-mlbf) colloid thruster is estimated since this thruster has not yet been fabricated. Testing of the high thrust colloid to date has been limited to a 1000-h test of a 1/12-size thruster.

(4) The 2.7-mN (600-μlbf) dual-beam cesium-contact thruster system offers some mass advantages over a monopropellant; however, its high power-to-thrust ratio penalizes this system.

(5) The 4.5-mN (1-mlbf) cesium bombardment thruster has been tested for only about 500 h; however, previous tests of a slightly larger thruster exceeded 8000 h. The 4.5-mN (1-mlbf) cesium bombardment thruster has promise of large total impulse life.

(6) The low-power MPD thruster was compared at a thrust and power point that unfortunately is accompanied with a low specific impulse. Higher-power operation places an excessive power penalty on the system. Development of an MPD with maximum performance at 1-mlbf thrust will make this thruster more attractive for north-south stationkeeping. The present optimum MPD thrust of 9 to 13 mN (2 to 3 mlbf) is attractive only for very large satellites.

(7) The experimental pulsed plasma thrusters are heavier in general than the ion and colloid thrusters but may offer more total impulse life.

(8) The total impulse of the pulsed plasma thruster is dependent on capacitor and gas injection valve technology. These thrusters are each plotted with an assumed life of 10^7 pulses per thruster and 2×10^7 pulses per capacitor. The figure of 10^7 pulses for the TRW pulsed inductive thruster is based on estimates of gas injection valve/spark gap life. The Fairchild Hiller thruster life is based on 2×10^7 discharges of a capacitor with specific mass of 22 J/kg (10 J/lbm). Without attainment of this assumed specific mass or an increase in the number of discharges possible, the high-energy pulsed plasma systems are noncompetitive on a mass basis.

These conclusions are based on mass, power, and performance considerations only and do not include thruster cost, reliability, and spacecraft/thruster interactions.

VII. Conclusions Based on Cost and Reliability

Cost and reliability are important factors in the selection of an auxiliary-propulsion system. There is not enough information on costs or component reliabilities to make detailed estimates of either cost or reliability of auxiliary electric thrusters, but qualitative estimates can be made.

Hardware cost of a microthruster system (one thruster with associated power conditioning) is approximately $100,000, while the hardware cost of a north-south stationkeeping thruster system is approximately $150,000. Flight qualification and thruster testing requirements really set the thruster costs. The extent of flight qualification and thruster testing will vary with the mission as well as the thruster.

Without component reliabilities based on sufficient test data, it is impossible to compute realistic quantitative reliabilities for electric thrusters. However, by comparing critical components and subsystems of electric thrusters, a qualitative reliability ranking (highest reliability listed first) can be estimated:

(1) Pulsed plasma, solid propellant

(2) Pulsed plasma, gaseous propellant

(3) Magnetoplasmadynamic (MPD)

(4) Ion

(5) Colloid

References

1. Goddard, R. H., "R. H. Goddard, An Autobiography," *Astronautics*, Vol. 4, p. 24, Apr. 1959.
2. Oberth, H., *Wege zur Raumschiffahrt*, R. Oldenbourg KG, Munich, 1929.
3. Stuhlinger, Ernst, *Ion Propulsion For Space Flight*, McGraw-Hill Book Co., Inc., New York, 1964.
4. Forrester, A. T., and Speiser, R. C., "Rocketdyne Internal Memorandum," RM 433191, to R. H. Boden, Aug. 1958.
5. Forrester, A. T. and Speiser, R. C., "Cesium-Ion Propulsion," *Astronautics*, Vol. 4, No. 10, p. 34, Oct. 1959.
6. Speiser, R. C., Dulgeroff, C. R., and Forrester, A. T., "Experimental Studies with Small Scale Ion Motors," ARS Preprint 926, presented at the 14th ARS Annual Meeting, Washington, D.C., Nov. 1959.
7. Naiditch, S., et al., "Ion Propulsion Systems: Experimental Studies," ARS Preprint 928-59, presented at the 14th ARS Annual Meeting, Washington, D.C., Nov. 1959.
8. Edwards, R. N., et al., "Experimental Studies of Cesium Ion Rocket Performance," ARS Paper 5, presented at the ARS Semi-Annual Meeting, Los Angeles, May 1960.
9. Sellen, J. M., and Shelton, H., "Space Change Measurements in Expanding Ion Beams," ARS Preprint 1160-60, May 1960.
10. Kaufman, H. R., and Reader, P. D., "Experimental Performance of Ion Rockets Employing Electron-Bombardment Ion Sources," from *Progress in Astronautics and Rocketry: Electrostatic Propulsion: Volume* V. Edited by D. B. Langmuir, E. Stuhlinger, and J. M. Sellen, Jr. Academic Press, New York, 1961.

References (contd)

11. Brewer, G. R., Etter, J. E., and Anderson, J. R., "Design and Performance of Small Ion Engines," ARS Preprint 1125-60, May 1960.

12. Langmuir, I., "The Effect of Space Change and Residual Gases on Thermionic Current in High Vacuum," *Phys. Rev.*, Vol. 2, p. 450, 1913.

    Taylor, J. B., and Langmuir, I., "The Evaporation of Atoms, Ions and Electrons from Cesium Films on Tungsten," *Phys. Rev.*, Vol. 44, p. 423, 1933.

13. Worlock, R., et al., "An Advanced Contact Ion Microthruster System," Paper 68-552, presented at the AIAA Fourth Propulsion Joint Specialist Conference, Cleveland, Ohio, June 1968.

14. Hunter, R. E., et al., "Cesium Contact Ion Microthruster Experiment Aboard Applications Technology Satellite (ATS)- IV," Paper 69-297, presented at the AIAA 7th Electric Propulsion Conference, Williamsburg, Virginia, Mar. 1969.

15. James, E. L., and Goldner, S. J., "Ion Engine Systems Testing," Air Force Technical Report AFAPL-TR-69-112, Feb. 1970.

16. Dulgeroff, C. R., Collett, C. R., and Simpkins, J. M., "Cesium Microthruster System," Paper 69-292, presented at the AIAA 7th Electric Propulsion Conference, Williamsburg, Virginia, Mar. 1969.

17. "Ion Microthruster System Design Report," Hughes Research Laboratories, Contract No. NAS5-12513, Malibu, Calif., Oct. 1969.

18. Anderson, J. R., "Performance of Ion Engines and Systems for Satellite Control," AIAA *Journal of Spacecraft and Rockets*, Vol. 3, No. 7, pp. 1086–1092, July 1966.

19. Anderson, J. R., and Thompson, S. A., "Development and Long-Life Performance of Ion Engines for Satellite Control," Paper 66-234, presented at the AIAA Fifth Electric Propulsion Conference, San Diego, California, Mar. 1966.

20. Sohl, G. et al., "Cesium Election-Bombardment Ion Microthrusters," *AIAA Journal of Spacecraft and Rockets*, Vol. 4, No. 9, pp. 1180–1183, Sep. 1967.

21. Fosnight, V. V., et al., "A Cesium Election-Bombardment Microthruster System," Paper 69-293, presented at the AIAA 7th Electric Propulsion Conference, Williamsburg, Virginia, Mar. 1969.

22. Worlock, R. M., et al., "Cesium Bombardment Ion Engine System Development," Air Force Technical Report, AFAPL-TR-69-87, Oct. 1969.

23. Sohl, G., Fosnight, V. V., and Goldner, S. J., "Election Bombardment Cesium Ion Engine System," EOS Report 6954 CR-54711, Dec. 1966.

24. James, E., et al., "A One Millipound Cesium Ion Thruster System," Paper 70-1149, presented at the AIAA 8th Electric Propulsion Conference, Stanford, California, Sep 1970.

25. Moore, R. D., "Magnets-Electrostatically Contained Plasma Ion Thruster," Paper 69-260, presented at the AIAA 7th Electric Propulsion Conference, Williamsburg, Virginia, Mar. 1969.

References (contd)

26. Reader, P. D., et al., "A Sub-Millipound Mercury Election-Bombardment Thruster," Paper 70-616, presented at the AIAA 6th Propulsion Joint Specialist Conference, San Diego, California, June 1970.

27. King, H. J. and Schnelker, D. E., "Thrust Vectoring Systems," Paper 70-1150, presented at the AIAA 8th Electric Propulsion Conference, Stanford, California, Sep. 1970

28. Banks, B. A., and Bechtel, R. T., "1000-Hour Endurance Test of A Glass-Coated Accelerator Grid On A 15-Centimeter-Diameter Kaufman Thruster," NASA TN D-5891, July 1970.

29. Bechtel, R. T., et al., "Effect of Facility Backsputtered Material On Performance of Glass-Coated Accelerator Grids for Kaufman Thrusters," AIAA paper 71-156, presented at the AIAA 9th Aerospace Sciences Meeting, New York, New York, Jan. 1971.

30. Masek, T. D., and Pawlik, E. V., "Thrust System Technology For Solar Electric Propulsion," Paper 68-541, presented at the AIAA 4th Propulsion Joint Specialist Conference, Cleveland, Ohio, June 1968.

31. Rawlin, V. K., and Kerslake, W. R., "SERT II: Durability of the Hollow Cathode and Future Applications of Hollow Cathodes," *AIAA Journal of Spacecraft and Rockets*, Vol. 7, No. 1, pp. 14–20, Jan. 1970.

32. Preston-Thomas, H., "Interorbital Transport Techniques," *Journal of British Interplanetary Society*, Vol. 11, p. 173, July 1952.

33. Schultz, R. D., *Some Technical Problems Associated With A Charged-Colloid Propulsion System*, Aerojet General Corporations Technical Memorandum 808, Sep. 1958.

    Schultz, R. D., and Weich, R. E. Jr., "Electric Propulsion with Colloidal Materials," presented at the AGARD Combustion and Propulsion Panel-Technical Meeting on "Advanced Propulsion Techniques," Pasadena, California, pp. 24–26, Aug. 1960.

34. Weich, R. E. Jr., *Heavy Particle Propulsion Research*, Thiokol Chemical Corp. Report, RMD-1155-S2, Denville, New Jersey, Dec. 1959.

35. Hunter, R. E., "Theoretical Consideration of Nonuniformly Charged Expellant Beams," ARL Tech. Note 60-138, Aeronautic Research Laboratory Air Force Research Division, Oct. 1960.

36. Hendricks, C. D., "Charged Droplet Experiments," *Journal of Colloid Science*, Vol. 17, pp. 249–259, 1962.

    Hendricks, C. D. and Pfeifer, R. J., "Parametric Studies of Electrohydrodynamic Spraying," Paper 66-252, presented at the AIAA Fifth Electric Propulsion Conference, San Diego, California, Mar. 1966.

37. Krohn, V. E., *Research on the Generation and Acceleration of Submicron-Size Particles*, Summary Report covering August 1959-February 1962, STL Report 8937-6005-cu-000.

References (contd)

Cohen, E., "STL Heavy Particle Propulsion Program," presented at the Third Symposium on Advanced Propulsion Concepts, Cincinnati, Ohio, Oct. 1962.

Cohen, E., *Research on the Electrostatic Generation and Acceleration of Submicron Size Particles*, Technical Report, ARL-63-88, May 1963.

38. Cohen, E., and Huberman, M. N., *Research on Charged Particle Electrostatic Thrusters*, Air Force Technical Report AFAPL-TR-66-94, Sep. 1966.

39. Hunter, R. E., and Wineland, S. H., "Exploration of the Feasibility of an Electrodeless Colloid Thruster Concept," presented at the Sixth International Symposium on Space Technology and Science, Tokyo, Japan, 1965.

40. Goldin, D. S., and Norgren, C. T., "Thrust Measurements of Colloidal Particles as an Indication of Particle Size and Thruster Operation," Paper 63-050, presented at the AIAA Electric Propulsion Conference, Colorado Springs, Colorado, Mar. 1963.

41. Perel, J., et al., "Research on a Charged Particle Bipolar Thruster," Paper 67-728, Sep. 1967.

42. Zafran, S., Beynon, J. C., and Cohen, E., "Colloid Microthruster System Development," Paper 68-84, presented at the AIAA Sixth Aerospace Sciences Meeting, New York, New York, Jan. 1968.

43. Kidd, P. W., *Research on the Bipolar Thruster*. Air Force Technical Report AFAPL-TR-67-110, Sep. 1967.

44. Huberman, M. N., and Kidd, P. W., *Charged Particle Electrostatic Thrusters*. Air Force Technical Report AFAPL-TR-69-14, Mar. 1969.

45. *Research and Development in Colloid Thruster Technology*. TRW Proposal No. 11882.000, Jan. 1969.

46. Zafran, S., et al., *Colloid Microthruster Experiment*, Air Force Technical Report AFAPL-TR-70-55, Aug. 1970.

47. Zafran, S., and Beynon, J. C., "Colloid Microthruster System Life Test," Paper 70-1110, presented at the AIAA 8th Electric Propulsion Conference, Stanford, California, Sep. 1970.

48. Burson, W. C., *Life Testing of A Colloid Thruster Source*, Air Force Technical Report AFAPL-TR-69-8, May 1969.

49. Shelton, H., et al., *Charged Droplet Electrostatic Thruster Systems*, Air Force Technical Report AFAPL-TR-70-31, June 1970.

50. Perel, J., Mahoney, J. F., and Yahiku, A. Y., "Analytical Study of Colloid Annular Thrusters," AIAA Paper 70-1113, presented at the AIAA 8th Electric Propulsion Conference, Stanford, California, August-September 1970.

51. Giannini, G. M., "The Plasma Jet and Its Application," Office of Scientific Research Technical Note 57-520, 1957.

52. Kantrowitz, A., "Introducing Magnetohydrodynamics," *Astronautics*, Vol. 3, No. 10, Oct., 1958.

References (contd)

53. John, R. R., Bennett, S., and Connors, J. F., "Arcjet Engine Performance: Experiment and Theory," *AIAA Journal*, Vol. 1, No. 11, pp. 2517–2525, Nov. 1963.

54. Ducati, A. C., et al., "1-KW Arcjet-Engine System-Performance Test," *AIAA Journal of Spacecraft and Rockets*, Vol 1, No. 3, pp. 327–332, May-June 1964.

55. Richter, R., "Investigation of Electrical Systems of Plasma Arc Jet Engines," AIAA paper 63-044, presented at the AIAA Electric Propulsion Conference, Colorado Springs, Colorado, Mar. 1963.

56. Clauser, M. U., "Magnetohydrodynamics," in *Space Technology*, Chapter 18. Edited by H. S. Seifert. John Wiley & Sons, Inc., New York, 1959.

57. Cann, G. L., and Marlotte, G. L., "Hall Current Plasma Accelerator," *AIAA Journal*, Vol. 2, No. 7, pp. 1234–1241, July 1964.

58. Ducati, A. C., *Study of the Factors Affecting the Efficiency in Thermal Acceleration of Propellants*, Sixth Quarterly Technical Report 6QS-113-1161. Giannini Scientific Corporation, Santa Ana, Calif., Oct. 1963.

59. *High Specific Impulse Thermo-Ionic Acceleration*, PRE-114-a. Giannini Scientific Corporation, Santa Ana, Calif., Dec. 1963.

60. Ducati, A. C., Giannini, G. M., and Muchlberger, E., "Experimental Results in High-Specific-Impulse Thermo-Ionic Acceleration," *AIAA Journal*, Vol. 2, No. 8, pp. 1452–1454, Aug. 1964.

61. John, R. R., and Bennett, S., *Arc Jet Technology Research and Development*, AVCO/RAD SR 64-239. AVCO Corporation, Research and Advanced Development Division (now AVSSD), Wilmington, Mass., Oct. 1954.

62. Cann, G. L., and Harder, R. L., *Follow-On Investigation of a Steady State Hall Current Accelerator*, Report 4010-Final. Electro-Optical System, Pasadena, Calif., Oct. 30, 1964. (Also available as NASA CR-54062.)

63. Patrick, R. M., and Schneiderman, A. M., *Study of Magnetic Annular Plasma Accelerator*, Summary Report, Contract NAS 3-5748, April 15, 1964 – Jan. 14, 1966. Avco-Everett Research Laboratory, Everett, Mass. (Also available as NASA CR-54686.)

64. Seikel, G. R., Bowditch, D. N. and Domitz, S., "Application of Magnetic-Expansion Plasma Thrusters to Satellite Station Keeping and Attitude Control Missions," Paper 64-677, presented at the AIAA Fourth Electric Propulsion Conference, Philadelphia, Pa., Aug. 1964.

65. Seikel, G. R., "Generation of Thrust-Electromagnet Thrusters," in *Electric Propulsion for Spacecraft*, pp. 19–24, NASA SP-22. National Aeronautics and Space Administration, Washington, D.C., 1962.

66. John, R. R., Bennett, S., and Jahn, R., "Current Status of Plasma Propulsion," AIAA Paper 66-565, presented at the AIAA Second Propulsion Joint Specialist Conference, Colorado Springs, Colorado, June 1966.

67. Burkhart, J., "Initial Performance Data On A Low-Power MPD Arc Thruster With A Downstream Cathode," AIAA Paper 70-1084, presented at the AIAA 8th Electric Propulsion Conference, Stanford, Calif., Aug. 1970.

References (contd)

68. Walker, E. L., and Seikel, G. R., Axisymmetric Expansion of a Plasma in a Magnetic Nozzle Including Thermal Conduction. NASA TN D-6154, Feb. 1971.

69. Burkhart, J., "Segmented Anode, CO_2-H_2 Performance and Hollow Cathode Erosion Tests on A Low Power MPD Arc Thruster," AIAA paper 69-242, presented at the AIAA 7th Electric Propulsion Conference, Williamsburg, Virginia, Mar. 1969.

70. Marshall, J., "Performance of a Hydromagnetic Plasma Gun," *Physics of Fluids*, Vol. 3, p. 134, 1960.

71. Maes, M. E., "The Confined Parallel Rail Pulsed Plasma Accelerator," ARS paper No. 2397-62, presented at the ARS Electric Propulsion Conference, Berkeley, Calif., Mar. 1962.

72. Kunen, A. E., McIlroy, W., "The Electromagnetic Pinch Effect for Space Propulsion." in *Dynamics of Conducting Gases*, pp. 179–189. Edited by A. B. Cambel & J. B. Fenn. (Northwestern University Press) Evanston, Ill. 1960.

73. Gloersen, P., "Pulsed Plasma Accelerators," ARS Paper No. 2129-61, presented at the ARS Space Flight Report to the Nation meeting, New York, Oct. 1961.

74. Gloersen, P., Gorowitz, B., and Kenney, J. T., "Energy Efficiency Trends in a Coaxial Gun Plasma Engine System," *AIAA Journal*, Vol. 4, No. 3, pp. 436–441, Mar. 1966.

75. Larson, A. V., et al., *Development of a Coaxial Plasma Gun for Space Propulsion*, Semiannual Report, Contract NAS3-7111, Nov. 1965.

76. Aronowitz, L., and Duclos, D. P., "Characteristics of the Pinch Discharge in a Pulsed Plasma Accelerator," in *Progress in Astronautics and Aeronautics: Volume IX, Electric Propulsion Development*, p. 513. Edited by E. Stuhlinger. Academic Press Inc., New York, 1963.

77. McIntosh, V. G., and Bostick, W. H., *A Button Source of Plasma*, University of California Lawrence Radiation Laboratories Report, UCRL-4688, Livermore, Calif., Apr. 1956.

78. Guman, W. J., and Peko, P. E., "Solid Propellant Pulsed Plasma Microthruster Studies," AIAA Paper 68-85, presented at the AIAA 6th Aerospace Sciences Meeting, New York, Jan. 1968.

79. LaRocca, A. V., "Solid Propellant Electric Thrusters for Attitude Control and Drift Correction of Space Vehicles," AIAA paper 66-229, presented at the AIAA Fifth Electric Propulsion Conference, San Diego, Calif., Mar. 1966.

80. Gilmour, A. J., "Concerning the Feasibility of A Vacuum Arc Thruster," AIAA paper 66-202, presented at the AIAA Fifth Electric Propulsion Conference, San Diego, Calif., Mar. 1966.

81. Dailey, C. L., "Investigation of Plasma Rotation In A Pulsed Inductive Accelerator," AIAA paper 68-86, presented at the AIAA 6th Aerospace Sciences Meeting, New York, Jan. 1968.

References (contd)

82. Sicotte, R. L., "RFI Measurements of UHF on a Pulsed Plasma Thruster," *AIAA Journal of Spacecraft and Rockets*, Vol. 7, No. 3, pp. 337–338, Mar. 1970.

83. Dolbec, R. E., "RFI Measurements on a LES-7 Prototype Pulsed Plasma Thruster," *AIAA Journal of Spacecraft and Rockets*, Vol. 7, No. 7, Engineering note, pp. 889-890, July 1970.

84. Guman, W. J., and Nathanson, D. M., "Pulsed Plasma Microthruster Propulsion System For Synchronous Orbit Satellite," AIAA paper 69-298, presented at the AIAA 7th Electric Propulsion Conference, Williamsburg, Virginia, Mar. 1969.

85. Braga-Illa, A. A., "The Future of Self-Contained Control of Synchronous Orbits," AIAA paper 70-479, presented at the AIAA 3rd Communications Satellite Systems Conference, Los Angeles, Calif., Apr. 6–8, 1970.

86. Vondra, R. J., Thomassen, K., and Solbes, A., "Analysis of Solid Teflon Pulsed Plasma Thruster," *AIAA Journal of Spacecraft and Rockets*, Vol. 7, No. 12, pp. 1402–1406, Dec. 1970.

87. Guman, W. J., Vondra, R. J., and Thomassen, K., "Pulsed Plasma Propulsion System Studies," AIAA paper 70-1148, presented at the AIAA 8th Electric Propulsion Conference, Stanford, Calif., Aug. 1970.

88. Guman, W., *Pulsed Plasma Technology in Microthruster*. AFAPL-TR-68-132, Air Force Aero Propulsion Lab., AFSC, Wright-Patterson AFB, Ohio, Nov. 1968.

89. LaRocca, A. V., and Perkins, G. S., "Pulsed Plasma Microthruster Applications and Techniques," AIAA paper 68-554, presented at the AIAA 4th Propulsion Joint Specialist Conference, Cleveland, Ohio, June 1968.

90. *Final Report Feasibility Assessment of a Solid Propellant Electric Thruster* (SPET), General Electric Report 66 SD 4255, General Electric Spacecraft Department, Mar. 15, 1966.

91. Lockwood, D. L., and Burdette, L. R., "A Pulsed Vacuum-Arc System Incorporating Throttle and Thrust Vector Controls," AIAA paper 70-180, presented at the AIAA 8th Aerospace Sciences Meeting, New York, Jan. 1970.

92. Jarrett, O., Hoell, J. M., and Lockwood, D. L., "Thrust Measurements On A Pulsed Vacuum-Arc Thruster," AIAA Paper No. 70-1146, presented at the AIAA 8th Electric Propulsion Conference, Stanford, Calif., Aug. 1970.

93. Gilmour, A. S., et al., "Recent Progress in Pulsed Vacuum-Arc Microthruster Research," AIAA paper 68-555, presented at the AIAA 4th Propulsion Joint Specialist Conference, Cleveland, Ohio, June 1968.

94. Dailey, C. L., *Thrust Measurement For A Pulsed Inductive Thruster*, TRW Systems Report AFOSR 70-0757TR, Air Force OSR Contract AF 44620-68-C-0042, Mar. 1970.

95. Benson, R. A., "Earth Orbital Mission Requirements for Secondary Propulsion Systems and Their Impact on Colloid Systems" ASME Paper No. 70-Av/SpT-31, presented at the ASME Space Technology and Heat Transfer Conference, Los Angeles, June 1970.